On the Diversity of Linear Transceivers in MIMO AF Relaying Systems

Changick Song, *Member IEEE* and Cong Ling, *Member IEEE*

***Abstract*—In this paper, we provide a comprehensive survey on designs and analyses of various relay-destination transceiving schemes such as zero-forcing (ZF), minimum mean squared error (MMSE), and maximum information rate (MIR) criteria in MIMO amplify-and-forward (AF) relaying systems. In the first part of the paper, we suggest a new framework for the transceiver designs utilizing a decomposable property of the error covariance matrix to give a general insight on the system and make the analysis more tractable. Then, in the second part of the paper, we provide an in-depth analysis on their diversity performance. Our analysis embraces two different scenarios, namely, the diversity-multiplexing tradeoff (DMT) and the diversity-rate tradeoff (DRT). First, we derive compact closed-form expressions for the DMT through tight upper and lower bounds. Then, we observe that while our DMT analysis accurately predicts performance of the ZF and MIR schemes, the MMSE-based designs exhibit a complicated rate dependent behavior, and thus are very unpredictable via DMT for finite rate cases. Thus, secondly, we highlight this interesting observation and characterize the diversity of the MMSE schemes at all finite rates. This leads to closed-form expressions for the DRT which reveals relationship between diversity, spectral efficiency, and the number of antennas at each node. The DRT analysis compliments our work on DMT, and thus the paper provides a complete understanding on the diversity of MIMO AF relaying systems.**

***Index Terms*—MIMO, relay, linear transceiver, MMSE, full-diversity, diversity-multiplexing tradeoff (DMT), diversity-rate tradeoff (DRT)**

I. Introduction

Recently, there has been growing interest in multiple-input multiple-output (MIMO) relaying techniques, due to combined benefits of improved link performance from MIMO channels and coverage extension from relaying techniques. In particular, although suboptimal, the amplify-and-forward (AF) schemes, which are represented in the base-band by transmit and receive combining matrices (namely transceiver), have attracted much attention for its low complexity implementation [1]–[7].

For example, when the maximum likelihood (ML) receiver is adopted at the destination, the transmit rate can be improved by adjusting the relay transceiver according to the maximum information rate (MIR) criterion [1] [2]. In contrast, when the decoding complexity is an issue, one may employ a linear equalizer at the destination such as the zero-forcing (ZF) or minimum mean squared error (MMSE) receivers, and then find appropriate transceivers at the relay to improve the performance [3]–[6]. In the meantime, to find operating points and predict their performance, analytical research on the transceiving schemes is also highly motivated. Several analytical studies have been made in literature [8]–[11] and references therein, but the performance has not been fully understood yet.

The *"diversity-multiplexing tradeoff"* (DMT) analysis provides a fundamental criterion to evaluate the performance of MIMO systems since it compactly characterizes the tradeoff between the rate and the block error probability in slow fading channels [12]. For this reason, a large amount of research has been conducted in MIMO relaying systems based on the DMT [13]–[20]. With the minimum mean squared error (MMSE) criterion, however, the DMT may be insufficient to characterize the diversity order, because the DMT framework, as an asymptotic notion in the high spectral efficiency and signal-to-noise ratio (SNR) regime, cannot distinguish between different spectral efficiencies belonging to the same multiplexing gain r.

Recently, it was shown in point-to-point (P2P) MIMO channels that although the DMT accurately predicts the diversity behavior of the MMSE receiver for the positive multiplexing gain ($r > 0$), the extrapolation of the DMT to the fixed rate scenarios, i.e., $r = 0$, is unable to predict the performance especially when a transmit rate falls below a certain threshold. This rate-dependent behavior of MMSE schemes has first been observed by Hedayat *et al.* in [21] and comprehensively analyzed by Mehana *et al.* in [22]. A similar phenomenon is observed in MIMO relaying systems, but an analysis has not been made so far.

In the first part of the paper, we introduce a unified framework for transceiver designs based on the error covariance decomposition (ECD) property of MIMO AF relaying systems. The ECD approach was first suggested in [4] for designing the MMSE transceiver under the assumption that the number of data-streams is smaller than or equal to the number of antennas at the relay and the destination. However, we would like to mention that any restriction on the antenna configuration is unnecessary under the MMSE strategy, because a certain diversity gain is always achievable as the rate becomes smaller, which will become clear in the analysis part of the paper (see Section IV). Therefore, it is important to provide a new ECD architecture that can be applied to any kinds of antenna configurations. We remark that our new approach not only

This work was supported in part by National Research Foundation of Korea funded by the Korea government (MSIP: Ministry of Science, ICT and Future Planning) under Grants NRF-2015R1C1A1A02036927 and in part by FP7 project PHYLAWS (EU FP7-ICT 317562).

This work was partially presented in IEEE International Symposium on Information Theory (ISIT) 2014.

C. Song is with the Department of Information and Communications Engineering, Korea National University of Transportaion, Chungju, Korea (e-mail: csong@ut.ac.kr).

C. Ling is with the Department of Electrical and Electronic Engineering, Imperial College, London, UK (e-mail: c.ling@imperial.ac.uk).

generalizes the previous work in [4], but also provides an ECD framework which brings various transceiving schemes such as the ZF, MMSE, and MIR strategies together.

In the second part of the paper, we present asymptotic analysis of the aforementioned linear transceivers. We first focus on the DMT performance of the systems. Previously, some DMT bounds have been found in [11] for the MMSE transceiver, but they are loose in general. In this paper, we identify an exact DMT expression of the ZF, MMSE, and MIR transceivers as a closed-form by obtaining tight upper and lower bounds. Our analysis also characterizes the DMT of the naive schemes where only a constant gain factor is applied at the relay without channel state information (CSI) to exhibit the effect of no CSI at the relay. The resulting DMT reveals that unlike the linear transceiving schemes whose DMT is given by a function of the number of relay antennas, the DMT of the naive schemes is determined by the minimum number of antennas of the relay and the destination. Therefore, as the number of relay antennas grows, the effect of the CSI at the relay will become more significant.

While our DMT analysis accurately predicts the ZF and MIR schemes, it is observed that when the rate is finite, the MMSE schemes exhibit a complicated rate dependent behavior, and thus are very unpredictable via DMT. To address this issue, we consider a constant rate transmission scheme over the SNR, i.e., $r = 0$ in MIMO AF relaying systems with linear transceivers. This leads to a closed-form expression for the *diversity-rate tradeoff* (DRT) which reveals the relationship between the diversity, spectral efficiency, and the number of antennas at each node. We note that under the DRT formulation, the analysis must be conducted more carefully compared to the DMT since certain ratios and terms that were simply ignored in the DMT analysis may be relevant. The proposed DRT bounds are tight except for some discontinuity rate points, and thus can precisely predict the diversity behavior of various MMSE relaying schemes.

It is interesting to observe that as the rate becomes smaller, the MMSE transceiver exhibits the ML-like performance [1] [2] with a full-diversity order of the MIMO relay channel. In contrast, the full-diversity may not be achievable by the naive-MMSE scheme no matter how small the rate is. The result suggests about the importance of the CSI at the relay for obtaining a proper DRT gain in MIMO relaying systems. Our DMT and DRT analyses are complementary to each other, and thus we obtain a complete understanding on the diversity of linear transceiving schemes over the MIMO AF relay channel. Finally, some simulations results are presented to demonstrate the accuracy of the analysis.

Notations: Throughout this paper, normal letters represent scalar quantities, boldface letters indicate vectors and boldface uppercase letters designate matrices. $\mathbf{I}_N$ is an $N \times N$ identity matrix We use $\mathbb{C}$ and $\mathbb{S}_+^M$ to denote a set of complex numbers and $M \times M$ positive definite matrices, respectively. $\preceq$ or $\succeq$ represent generalized inequality defined on the positive definite cone. In addition, $E[\cdot]$, $(\cdot)^H$, $(\cdot)^+$, $\lceil \cdot \rceil$, and $\lfloor \cdot \rfloor$ stand for expectation, conjugate transpose, $\max(\cdot, 0)$, rounding up, and down operations, respectively. $[\mathbf{A}]_{k,k}$ and $\mathrm{Tr}\,(\mathbf{A})$ denote the k-th diagonal element and trace function of a matrix $\mathbf{A}$. The k-th element of a vector $\mathbf{a}$ is denoted by a_k. We denote $f(\rho) \doteq g(\rho)$, when two functions $f(\rho)$ and $g(\rho)$ are exponentially equal as $\lim_{\rho\to\infty} \frac{\log f(\rho)}{\log \rho} = \lim_{\rho\to\infty} \frac{\log g(\rho)}{\log \rho}$. Inequalities $\dot{\leq}$ and $\dot{\geq}$ are similarly defined.

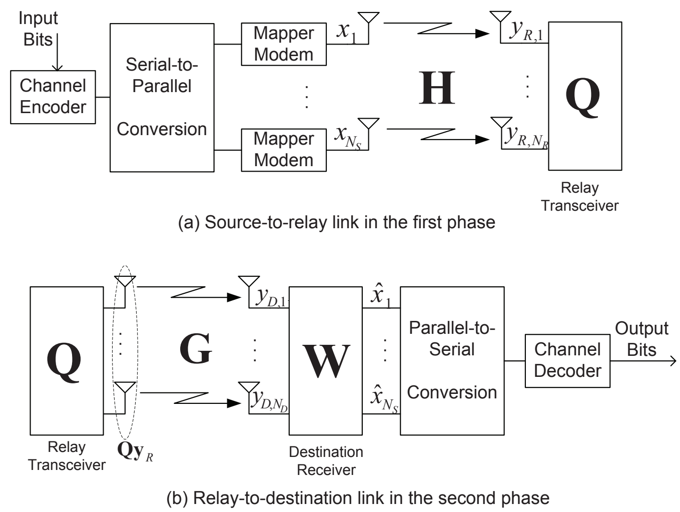

Fig. 1. Joint encoding/decoding structure for MIMO AF relaying channels with linear transceivers

II. System Model

In this paper, we consider quasi-static flat fading MIMO AF relaying channels equipped with N_S, N_R, and N_D number of antennas at the source, the relay, and the destination, respectively. A direct link between the source and the destination is ignored due to large pathloss. We assume that no channel state information (CSI) is available at the source, but perfect knowledge of both $\mathbf{H}$ and $\mathbf{G}$, which is often referred to as the global CSI, is allowed at the destination. The relay can be informed of either the global CSI or no CSI.

Figure 1 shows a two-hop relaying architecture where linear transceivers $\mathbf{Q}$ and $\mathbf{W}$ are adopted at the relay and the destination, respectively. The relay may operate in either half-duplex or full duplex, but to avoid a loop interference at the relay, we assume the half-duplex relay which requires two separate phases for each data transmission. Note that if the relay can remove the loop interference completely, the full-duplex rate becomes simply twice the half-duplex one.

and then the output of the underlying MIMO channel between the source and the relay is expressed as $\mathbf{y}_R = \mathbf{H}\mathbf{x} + \mathbf{n}_R$, where $\mathbf{x} \in \mathbb{C}^{N_S \times 1}$, $\mathbf{H} \in \mathbb{C}^{N_R \times N_S}$ and $\mathbf{n}_R \in \mathbb{C}^{N_R \times 1}$ represent the input signal vector, the channel matrix between the source and the relay, and the noise vector at the relay, respectively. Denoting the total transmit power at the source by P_S, each source antenna uses equal power $\rho \triangleq E[|x_k|^2] = P_S/N_S$ for all k.

In the second phase, the relay signal $\mathbf{y}_R$ is amplified by the relay matrix $\mathbf{Q} \in \mathbb{C}^{N_R \times N_R}$ and transmitted to the destination. Then, the standard baseband signal at the destination is written by

$$\mathbf{y}_D = \mathbf{G}\mathbf{Q}\mathbf{y}_R + \mathbf{n}_D = \mathbf{G}\mathbf{Q}\mathbf{H}\mathbf{x} + \mathbf{G}\mathbf{Q}\mathbf{n}_R + \mathbf{n}_D, \quad (1)$$

where $\mathbf{G}$ and $\mathbf{n}_D$ designate the second-hop channel matrix and the noise vector at the destination. The relay matrix $\mathbf{Q}$ satisfies a constraint $E[\|\mathbf{Q}\mathbf{y}_R\|^2] \leq P_R$ where P_R designates the total power budget at the relay. Finally, when a linear equalizer $\mathbf{W} \in \mathbb{C}^{N_S \times N_D}$ is employed at the destination, the estimated signal waveform $\hat{\mathbf{x}} \in \mathbb{C}^{N_S \times 1}$ is expressed as $\hat{\mathbf{x}} = \mathbf{W}\mathbf{y}_D$.

As the equalizer $\mathbf{W}$ decouples the received signal into N_S parallel data streams, the transmit signals at the source can be encoded either jointly or separately. To be specific, the joint encoding indicates the case in which a single channel encoder supports all the data streams at the source so that coding is applied jointly across antennas as illustrated in Figure 1. Hence, this coding scheme is advantageous to attain a diversity gain of MIMO channels. In contrast, the separate encoding drives N_S data streams independently using N_S encoders, the outputs of which are fed into N_S independent decoders; thus, is based sorely on spatial multiplexing.

In this work, we make a standard assumption that all entries of channel matrices $\mathbf{H}$ and $\mathbf{G}$ are independent and identically distributed (i.i.d.) $\sim \mathcal{CN}(0,1)$ and remain constant during the transmission of a codeword. All elements of the noise vectors $\mathbf{n}_R$ and $\mathbf{n}_D$ are also i.i.d. Gaussian $\sim \mathcal{CN}(0,1)$. We will use the following eigenvalue decompositions $\mathbf{H}^H\mathbf{H} = \mathbf{U}_h\mathbf{\Lambda}_h\mathbf{U}_h^H$ and $\mathbf{G}^H\mathbf{G} = \mathbf{U}_g\mathbf{\Lambda}_g\mathbf{U}_g^H$, where $\mathbf{U}_h \in \mathbb{C}^{N_S \times N_S}$ and $\mathbf{U}_g \in \mathbb{C}^{N_R \times N_R}$ are unitary matrices, and $\mathbf{\Lambda}_h \in \mathbb{C}^{N_S \times N_S}$ and $\mathbf{\Lambda}_g \in \mathbb{C}^{N_R \times N_R}$ represent square diagonal matrices with non-negative eigenvalues $\lambda_{h,i}$ for $i = 1, \ldots, N_S$ and $\lambda_{g,j}$ for $j = 1, \ldots, N_R$, respectively. All eigenvalues are arranged in descending order. Throughout the paper, $M = \min(N_S, N_R)$ and $N = \min(N_S, N_R, N_D)$.

III. Optimal Transceiver Designs

In this section, we design the optimal relay matrix (transceiver) with various design criteria, e.g., ZF, MMSE, and MIR. Recently, the authors in [1] and [3] have developed the MIR and MMSE transceivers, respectively based on the singular-value decomposition (SVD) techniques. However, the conventional SVD approaches produce a complicated compound channel matrix and colored noise at the destination which are difficult to deal with. In this section, we introduce an alternative design method utilizing the ECD property, which makes the analysis more tractable. Our approach extends the previous result in [4] so that it can be applied to any kind of antenna configurations and provides a useful design framework which brings the ZF, MMSE, and MIR strategies together.

A. MMSE Transceiver

Define the error vector $\mathbf{e} \triangleq \hat{\mathbf{x}} - \mathbf{x}$ and its covariance matrix $\mathbf{R}_e \triangleq E[\mathbf{e}\mathbf{e}^H]$. Then, the joint MMSE optimization problem for $\mathbf{Q}$ and $\mathbf{W}$ is written by

$$\begin{aligned} &\min_{\mathbf{Q},\mathbf{W}} \text{Tr}\,(\mathbf{R}_e) \\ &s.t. \;\; \text{Tr}\left(\mathbf{Q}(\rho\mathbf{H}\mathbf{H}^H + \mathbf{I}_{N_R})\mathbf{Q}^H\right) \leq P_R. \end{aligned} \tag{2}$$

For a given $\mathbf{Q}$, the optimal destination receiver is given by the Wiener filter solution as [23]

$$\hat{\mathbf{W}}_{\text{wf}} = \rho\mathbf{H}^H\mathbf{Q}^H\mathbf{G}^H(\rho\mathbf{G}\mathbf{Q}\mathbf{H}\mathbf{H}^H\mathbf{Q}^H\mathbf{G}^H + \mathbf{R}_v)^{-1}, \tag{3}$$

where $\mathbf{R}_v \triangleq \mathbf{G}\mathbf{Q}\mathbf{Q}^H\mathbf{G}^H + \mathbf{I}_{N_D}$ designates the covariance matrix of the effective noise $\mathbf{v} \triangleq \mathbf{G}\mathbf{Q}\mathbf{n}_R + \mathbf{n}_D$.

Meanwhile, for a given $\mathbf{W} = \hat{\mathbf{W}}_{\text{wf}}$ in (3), the error covariance matrix $\mathbf{R}_e$ becomes [4]

$$\mathbf{R}_e(\mathbf{Q}) = (\mathbf{H}^H\mathbf{Q}^H\mathbf{G}^H\mathbf{R}_v^{-1}\mathbf{G}\mathbf{Q}\mathbf{H} + \rho^{-1}\mathbf{I}_{N_s})^{-1}, \tag{4}$$

which implies that a principal issue of the problem (2) is now to find $\mathbf{Q}$. The following lemma shows that with the MMSE strategy, the optimal relay matrix takes a particular structure.

Lemma 1: The optimal relay matrix $\mathbf{Q}$ of the problem (2) is generally expressed as a product of two matrices

$$\hat{\mathbf{Q}} = \mathbf{B}\mathbf{L}, \tag{5}$$

where $\mathbf{B} \in \mathbb{C}^{N_R \times N_S}$ is an arbitrary matrix and $\mathbf{L} \in \mathbb{C}^{N_S \times N_R}$ represents a matrix which is given by $\mathbf{L} = \mathbf{P}\mathbf{H}^H$ with $\mathbf{P} \in \mathbb{C}^{N_S \times N_S}$ being a square invertible matrix.

Proof: In general, one can write $\mathbf{Q}$ in a general form as $\mathbf{Q} = \mathbf{Q}_\parallel + \mathbf{Q}_\perp$ where $\mathbf{Q}_\parallel$ and $\mathbf{Q}_\perp$ denote the components of $\mathbf{Q}$ such that the row space of $\mathbf{Q}_\parallel$ and $\mathbf{Q}_\perp$ are parallel and orthogonal to the column space of $\mathbf{H}$, respectively. Then, from the error covariance matrix $\mathbf{R}_e$ in (4) and the relay power consumption in (2), it is easy to verify that

$$\begin{aligned} \mathbf{R}_e(\mathbf{Q}_\parallel) &\preceq \mathbf{R}_e(\mathbf{Q}) \\ \text{Tr}(\mathbf{Q}_\parallel(\rho\mathbf{H}\mathbf{H}^H + \mathbf{I}_{N_R})\mathbf{Q}_\parallel^H) &\leq \text{Tr}(\mathbf{Q}(\rho\mathbf{H}\mathbf{H}^H + \mathbf{I}_{N_R})\mathbf{Q}^H). \end{aligned}$$

With these results, we now confirm that the optimal relay matrix only contains the parallel components to the column space of $\mathbf{H}$, i.e., $\hat{\mathbf{Q}} = \mathbf{Q}_\parallel$ that can be generally expressed as $\mathbf{Q}_\parallel = \overline{\mathbf{B}}\mathbf{H}^H$ for any matrix $\overline{\mathbf{B}} \in \mathbb{C}^{N_R \times N_S}$, because the row space of $\mathbf{H}^H$ constitutes that of $\mathbf{Q}_\parallel$. Now, let us define $\mathbf{P} \in \mathbb{C}^{N_S \times N_S}$ as an arbitrary square invertible matrix. Then, the optimal relay matrix is further expandable to $\hat{\mathbf{Q}} = \mathbf{B}\mathbf{P}\mathbf{H}^H$ for any matrix $\mathbf{B} \in \mathbb{C}^{N_R \times N_S}$, and we obtain Lemma 1. ■

From now on, we refer to $\mathbf{L}$ and $\mathbf{B}$ as a relay receiver and a relay precoder, respectively. Let us set $\mathbf{P} = (\mathbf{H}^H\mathbf{H} + \rho^{-1}\mathbf{I}_{N_S})^{-1}$ so that $\mathbf{L}$ forms the MMSE receiver for the first-hop channel $\mathbf{H}$ with the input signal $\mathbf{x}$. Also, we define a relay signal $\mathbf{y} \triangleq \mathbf{L}\mathbf{y}_R \in \mathbb{C}^{N_S \times 1}$ which in turn becomes an input signal to the relay precoder $\mathbf{B}$ and its covariance matrix $\mathbf{R}_y \triangleq E[\mathbf{y}\mathbf{y}^H] \in \mathbb{C}^{N_S \times N_S}$ which is given by

$$\mathbf{R}_y = \mathbf{L}(\rho\mathbf{H}\mathbf{H}^H + \mathbf{I}_{N_R})\mathbf{L}^H = \rho\mathbf{H}^H\mathbf{H}(\mathbf{H}^H\mathbf{H} + \rho\mathbf{I}_{N_S})^{-1}. \tag{6}$$

Now, the estimated signal vector $\hat{\mathbf{x}}$ and the relay power constraint in (2) are rephrased by

$$\hat{\mathbf{x}} = \mathbf{W}(\mathbf{G}\mathbf{B}\mathbf{y} + \mathbf{n}_D) \;\; \text{and} \;\; \text{Tr}(\mathbf{B}\mathbf{R}_y\mathbf{B}^H) \leq P_R, \tag{7}$$

respectively. However, a careful examination of (6) reveals that the rank of $\mathbf{R}_y$ equals $M \triangleq \min(N_S, N_R)$, which means that $\mathbf{R}_y$ is non-invertible when $N_S > N_R$. This fact makes the analysis more challenging, but has not been fully addressed in conventional literature.

In the following, we revisit the previous works in [3] and [4], and provide more general and insightful designs without restriction on the number of antennas (or data streams) at the source. In fact, when the relay receiver $\mathbf{L}$ forms the MMSE receiver for the first hop channel, one can show that the error covariance matrix $\mathbf{R}_e$ in (4) is expressed as a sum of two individual covariance matrices, each of which represents the first hop and the second hop MIMO channels, respectively. This result has been proved in [4], but the proof was limited to the cases of $N_S \leq \min(N_R, N_D)$. For the sake of completeness, we give a new result of error decomposition that can be applied to any kind of antenna configurations.

Lemma 2: Define the eigenvalue decomposition $\mathbf{R}_y = \mathbf{U}_h \mathbf{\Lambda}_y \mathbf{U}_h^H$ *where* $\mathbf{\Lambda}_y \in \mathbb{C}^{N_S \times N_S}$ *represents a square diagonal matrix with eigenvalues* $\lambda_{y,k}$ *for* $k = 1, \dots, N_S$ *arranged in descending order. Then, without loss of MMSE optimality, the error covariance matrix* $\mathbf{R}_e$ *equals*

$$\begin{aligned} \mathbf{R}_e(\mathbf{B}) \;=\; & (\mathbf{H}^H\mathbf{H} + \rho^{-1}\mathbf{I}_{N_S})^{-1} \\ & + \widetilde{\mathbf{U}}_h \big(\widetilde{\mathbf{U}}_h^H \mathbf{B}^H \mathbf{G}^H \mathbf{G} \mathbf{B} \widetilde{\mathbf{U}}_h + \widetilde{\mathbf{\Lambda}}_y^{-1}\big)^{-1} \widetilde{\mathbf{U}}_h^H \end{aligned} \quad (8)$$

where $\widetilde{\mathbf{U}}_h \in \mathbb{C}^{N_S \times M}$ *is a matrix constructed by the first* M *columns of* $\mathbf{U}_h$ *and* $\widetilde{\mathbf{\Lambda}}_y$ *indicates the* $M \times M$ *upper-left submatrix of* $\mathbf{\Lambda}_y$.

Proof: As the relay receiver $\mathbf{L}$ follows the receive Wiener filter structure, its output signal $\mathbf{y}$ must satisfy the orthogonality principle [24], i.e., $E\left[(\mathbf{y} - \mathbf{x})\mathbf{y}^H\right] = \mathbf{0}$. Meanwhile, using $\mathbf{y}$, the MSE can be expressed as $E\left[\|\mathbf{e}\|^2\right] = E\left[\|\hat{\mathbf{x}} - \mathbf{y} + \mathbf{y} - \mathbf{x}\|^2\right]$. Then, due to the orthogonality principle above, it is true that the signal $\mathbf{y} - \mathbf{x}$ becomes orthogonal to $\hat{\mathbf{x}}$ as well as $\mathbf{y}$, since $\hat{\mathbf{x}} = \mathbf{W}\mathbf{y}_D = \mathbf{W}(\mathbf{G}\mathbf{B}\mathbf{y} + \mathbf{n}_D)$ is also a function of $\mathbf{y}$ and independent noise $\mathbf{n}_D$. Therefore, we have

$$E\left[\|\mathbf{e}\|^2\right] = \mathrm{MSE}_H + \mathrm{MSE}_G, \quad (9)$$

where we define $\mathrm{MSE}_H \triangleq E\big[\|\mathbf{y} - \mathbf{x}\|^2\big]$ and $\mathrm{MSE}_G \triangleq E\big[\|\mathbf{W}\mathbf{y}_D - \mathbf{y}\|^2\big]$.

In what follows, we will show that MSE_H and MSE_G in (9) can be expressed as matrix forms like the first and second terms in (8), respectively. Let us first take a look at MSE_G. In this case, i.e., for given $\mathbf{Q} = \mathbf{B}\mathbf{L}$, the optimal destination receiver (3) is rephrased by $\hat{\mathbf{W}}_{\mathrm{WF}} = \mathbf{R}_y \mathbf{B}^H \mathbf{G}^H (\mathbf{G}\mathbf{B}\mathbf{R}_y\mathbf{B}^H\mathbf{G}^H + \mathbf{I}_{N_d})^{-1}$ which amounts to the MMSE estimator for the virtual input signal $\mathbf{y}$ at the relay. Thus, it follows

$$\begin{aligned} \mathrm{MSE_G} &= E\left[\mathrm{Tr}\big((\hat{\mathbf{W}}_{\mathrm{WF}}\mathbf{y}_D - \mathbf{y})(\hat{\mathbf{W}}_{\mathrm{WF}}\mathbf{y}_D - \mathbf{y})^H\big)\right] \\ &= \mathrm{Tr}\big(\mathbf{R}_y - \mathbf{R}_y\mathbf{B}^H\mathbf{G}^H(\mathbf{G}\mathbf{B}\mathbf{R}_y\mathbf{B}^H\mathbf{G}^H + \mathbf{I}_{N_D})^{-1}\mathbf{G}^H\mathbf{B}^H\mathbf{R}_y\big). \end{aligned}$$

We now expand the matrix $\mathbf{B}$ to a more general form as $\mathbf{B} = \breve{\mathbf{B}}\mathbf{U}_h^H$ where $\breve{\mathbf{B}} = [\mathbf{B}_1 \;\, \mathbf{B}_2]$ with $\mathbf{B}_1 \in \mathbb{C}^{N_R \times M}$ and $\mathbf{B}_2 \in \mathbb{C}^{N_R \times (N_S - M)}$. Since $\mathbf{R}_y$ is a rank-M matrix, setting $\mathbf{B}_2 = \mathbf{0}$ has no impact on both the MSE and the relay power consumption in (7). Therefore, without loss of generality, $\mathrm{MSE_G}$ in (9) is further rephrased by

$$\begin{aligned} \mathrm{MSE_G} \;=\; & \mathrm{Tr}\big(\widetilde{\mathbf{U}}_h(\widetilde{\mathbf{\Lambda}}_y - \widetilde{\mathbf{\Lambda}}_y^H\mathbf{B}_1^H\mathbf{G}^H \\ & \times(\mathbf{G}\mathbf{B}_1\widetilde{\mathbf{\Lambda}}_y\mathbf{B}_1^H\mathbf{G}^H + \mathbf{I}_{N_D})^{-1}\mathbf{G}^H\mathbf{B}_1^H\widetilde{\mathbf{\Lambda}}_y)\widetilde{\mathbf{U}}_h^H\big) \\ =\; & \widetilde{\mathbf{U}}_h\big(\mathbf{B}_1^H\mathbf{G}^H\mathbf{G}\mathbf{B}_1\widetilde{\mathbf{U}}_h + \widetilde{\mathbf{\Lambda}}_y^{-1}\big)^{-1}\widetilde{\mathbf{U}}_h^H \\ =\; & \widetilde{\mathbf{U}}_h\big(\widetilde{\mathbf{U}}_y^H\mathbf{B}^H\mathbf{G}^H\mathbf{G}\mathbf{B}\widetilde{\mathbf{U}}_h + \widetilde{\mathbf{\Lambda}}_y^{-1}\big)^{-1}\widetilde{\mathbf{U}}_h^H, \end{aligned}$$

where the last equality follows from $\mathbf{B}_1 = \mathbf{B}\widetilde{\mathbf{U}}_h$. Meanwhile, MSE_H is equivalent to one in the conventional P2P MMSE systems; thus, the proof simply follows from the previous results in [25] and the proof is completed. ■

The result of Lemma 2 reveals that we need to optimize only the second MSE term with respect to $\mathbf{B}$ because the first term of $\mathbf{R}_e$ consists of known parameters. The standard theory of MMSE filter designs [3] [26] shows that in this case, the optimal $\mathbf{B}$ can be written in general by $\hat{\mathbf{B}} = \widetilde{\mathbf{U}}_g\mathbf{\Phi}\widetilde{\mathbf{U}}_h^H$ where $\widetilde{\mathbf{U}}_g \in \mathbb{C}^{N_R \times M}$ denotes a matrix constructed by the first M columns of $\mathbf{U}_g$ and $\mathbf{\Phi} \in \mathbb{C}^{M \times M}$ is an arbitrary matrix. Finally, substituting $\hat{\mathbf{B}}$ into (8), the modified problem determines the optimal $\mathbf{\Phi}$:

$$\begin{aligned} \hat{\mathbf{\Phi}} \;=\; & \arg\min_{\mathbf{\Phi}} \mathrm{Tr}\left(\big(\mathbf{\Phi}\widetilde{\mathbf{\Lambda}}_g\mathbf{\Phi}^H + \widetilde{\mathbf{\Lambda}}_y^{-1}\big)^{-1}\right) \\ & \textit{s.t.} \quad \mathrm{Tr}(\mathbf{\Phi}\widetilde{\mathbf{\Lambda}}_y\mathbf{\Phi}^H) \leq P_R \end{aligned} \quad (10)$$

with $\widetilde{\mathbf{\Lambda}}_g$ representing the $M \times M$ upper-left submatrix of $\mathbf{\Lambda}_g$. It is known that for $\mathbf{A}$ and $\mathbf{B} \in \mathbb{S}_+^M$, we have $\mathrm{Tr}(\mathbf{A}^{-1}) \geq \sum_{i=1}^M ([\mathbf{A}]_{k,k})^{-1}$ and $\mathrm{Tr}(\mathbf{A}\mathbf{B}) \geq \sum_{i=1}^M \lambda_i(\mathbf{A})\lambda_{M-i+1}(\mathbf{B})$ [27]. From these results, it is immediate that the minimum MSE is achieved when $\mathbf{\Phi}$ is a diagonal matrix and the resulting problem simply becomes convex; thus, can be easily solved by Karush-Kuhn-Tucker conditions [23]. In combination with the relay receiver $\mathbf{L}$ in (5), we finally have

$$\hat{\mathbf{Q}} = \hat{\mathbf{B}}\mathbf{L} = \widetilde{\mathbf{U}}_g\hat{\mathbf{\Phi}}\widetilde{\mathbf{U}}_h^H\mathbf{L}, \quad (11)$$

where the k-th diagonal element of $\hat{\mathbf{\Phi}}$ denoted by $\hat{\phi}_k$ is given by $|\hat{\phi}_k|^2 = (\lambda_{y,k}\lambda_{g,k})^{-1}\left(\nu(\lambda_{y,k}\lambda_{g,k})^{1/2} - 1\right)^+$ for $k = 1, 2, \dots, M$ with ν being chosen to satisfy the relay power constraint in (7). Note that if $\lambda_{g,k} = 0$, we have $|\hat{\phi}_k|^2 = 0$.

B. ZF Transceiver

To achieve the MMSE transceiver, the relay needs to measure noise power at the destination, which requires an additional feedback information from the destination to the relay. Therefore, in some practical systems with limited control channels between the relay and the destination, system designs based on the ZF strategy may be useful. Nevertheless, to the best of our knowledge, the ZF transceiver optimization in MIMO AF relaying systems has not been considered so far. In this section, we show that the optimal solutions for the ZF schemes are also attainable with our ECD framework.

The ZF problem arises from the constraint that $\hat{\mathbf{x}}$ is an interference-free estimation of $\mathbf{x}$. Thus, the optimization problem can be formulated as [25]

$$\begin{aligned} \min_{\mathbf{Q},\mathbf{W}} \;\; & \mathrm{Tr}\left(\mathbf{R}_e\right) \\ \textit{s.t.} \;\; & \mathrm{Tr}\left(\mathbf{Q}(\rho\mathbf{H}\mathbf{H}^H + \mathbf{I}_{N_R})\mathbf{Q}^H\right) \leq P_R \quad (12) \\ & \mathbf{W}\mathbf{R}_v^{-1/2}\mathbf{G}\mathbf{Q}\mathbf{H} = \mathbf{I}. \quad (13) \end{aligned}$$

We notice that the ZF problem is only defined when $N_S \leq \min(N_R, N_D)$ due to the ZF constraint (13). Then, the solution for the destination receiver is simply given by

$$\hat{\mathbf{W}}_{\mathrm{zf}} = (\mathbf{H}^H\mathbf{Q}^H\mathbf{G}^H\mathbf{R}_v^{-1}\mathbf{G}\mathbf{Q}\mathbf{H})^{-1}\mathbf{H}^H\mathbf{Q}^H\mathbf{G}^H\mathbf{R}_v^{-\frac{1}{2}}.$$

Once $\hat{\mathbf{W}}_{\mathrm{zf}}$ is given, the constraint (13) can be removed, which means that the remaining problem for $\mathbf{Q}$ amounts to the standard MMSE problem (2). It is thus clear from Lemma 1 that by setting $\mathbf{P} = (\mathbf{H}^H\mathbf{H})^{-1}$, the optimal relay matrix can be expressed as $\hat{\mathbf{Q}} = \mathbf{B}\mathbf{L}_z$ where $\mathbf{L}_z = (\mathbf{H}^H\mathbf{H})^{-1}\mathbf{H}^H$ represents the ZF receiver for the first-hop channel $\mathbf{H}$, while $\mathbf{B}$ is an unknown matrix as of yet.

Now, let us apply the results of $\hat{\mathbf{W}}_{\text{zf}}$ and $\hat{\mathbf{Q}}$ to the problem (12). Then, the error covariance matrix is

$$\begin{aligned}
\mathbf{R}_e &= \big(\mathbf{H}^H\hat{\mathbf{Q}}^H\mathbf{G}^H(\mathbf{G}\hat{\mathbf{Q}}\hat{\mathbf{Q}}^H\mathbf{G}^H + \mathbf{I}_{N_D})^{-1}\mathbf{G}\hat{\mathbf{Q}}\mathbf{H}\big)^{-1}\\
&= \Big(\mathbf{B}^H\mathbf{G}^H\big(\mathbf{G}\mathbf{B}(\mathbf{H}^H\mathbf{H})^{-1}\mathbf{B}^H\mathbf{G}^H + \mathbf{I}_{N_D}\big)^{-1}\mathbf{G}\mathbf{B}\Big)^{-1}\\
&= \Big(\mathbf{B}^H\mathbf{G}^H\big(\mathbf{I}_{N_D} - \mathbf{G}\mathbf{B}(\mathbf{H}^H\mathbf{H} + \mathbf{B}^H\mathbf{G}^H\mathbf{G}\mathbf{B})^{-1}\\
&\qquad\qquad \times\mathbf{B}^H\mathbf{G}^H\big)^{-1}\mathbf{G}\mathbf{B}\Big)^{-1}\\
&= \Big(\mathbf{B}^H\mathbf{G}^H\mathbf{G}\mathbf{B} - \mathbf{B}^H\mathbf{G}^H\mathbf{G}\mathbf{B}\\
&\qquad \times\big(\mathbf{H}^H\mathbf{H} + \mathbf{B}^H\mathbf{G}^H\mathbf{G}\mathbf{B}\big)^{-1}\mathbf{B}^H\mathbf{G}^H\mathbf{G}\mathbf{B}\Big)^{-1}\\
&= \big(\mathbf{H}^H\mathbf{H}\big)^{-1} + \big(\mathbf{B}^H\mathbf{G}^H\mathbf{G}\mathbf{B}\big)^{-1}. \qquad (14)
\end{aligned}$$

Similar to (7), the relay power constraint is modified as $\text{Tr}(\mathbf{B}\mathbf{R}_z\mathbf{B}^H) \leq P_R$ where $\mathbf{R}_z$ indicates the covariance matrix of the relay signal $\mathbf{z} = \mathbf{L}_z\mathbf{y}_R$, which is given by

$$\mathbf{R}_z \triangleq \mathbf{L}_z(\rho\mathbf{H}\mathbf{H}^H + \mathbf{I}_{N_R})\mathbf{L}_z^H. \qquad (15)$$

Accordingly, the error covariance decomposition method holds for the ZF systems as well.

By equation (14), we obtain the modified problem to find $\mathbf{B}$ as

$$\min_{\mathbf{B}} \text{Tr}\Big(\big(\mathbf{B}^H\mathbf{G}^H\mathbf{G}\mathbf{B}\big)^{-1}\Big) \quad s.t. \quad \text{Tr}(\mathbf{B}\mathbf{R}_z\mathbf{B}^H) \leq P_R.$$

Similar to (10), we set $\hat{\mathbf{B}} = \widetilde{\mathbf{U}}_g\mathbf{\Phi}\mathbf{U}_h^H$ with $\mathbf{\Phi}_z \in \mathbb{C}^{N_S\times N_S}$ being a square diagonal matrix. Then, the remaining steps simply follow the result in Section III-A. Finally, we obtain the optimal relay matrix as $\hat{\mathbf{Q}} = \widetilde{\mathbf{U}}_g\hat{\mathbf{\Phi}}\mathbf{U}_h\mathbf{L}_z$ where the k-th diagonal element of $\hat{\mathbf{\Phi}}$ denoted by $\hat{\phi}_k$ is given by $|\hat{\phi}_k|^2 = \sqrt{\frac{\mu}{\lambda_{z,k}\lambda_{g,k}}}$ for $k = 1, 2, \ldots, N_S$, the eigenvalues of $\mathbf{R}_z$ are $\lambda_{z,1} > \cdots > \lambda_{z,N_S}$, and μ is chosen to satisfy the relay power constraint. Note that if $\lambda_{g,k} = 0$, we have $|\hat{\phi}_k|^2 = 0$.

C. MIR Transceiver

In this subsection, we reinterpret the conventional MIR design in [1] and [2] with our ECD framework for the sake of completeness and ease of analysis. Provided that the destination adopts the ML receiver with the optimal Gaussian codewords, the MIR transceiver at the relay is obtained by solving the following problem

$$\begin{aligned}
\max_{\mathbf{Q}} \mathcal{I}(\mathbf{Q}) &= \frac{1}{\eta}\log\left|\rho\mathbf{R}_e^{-1}(\mathbf{Q})\right|\\
&= \frac{1}{\eta}\log\left|\rho\mathbf{H}^H\mathbf{Q}^H\mathbf{G}^H\mathbf{R}_v^{-1}\mathbf{G}\mathbf{Q}\mathbf{H} + \mathbf{I}_{N_S}\right| \quad (16)
\end{aligned}$$

with the power constraint in (2). The pre-log factor $1/\eta$ represents the duplexing scheme employed at the relay, e.g., $\eta = 1$ for the full-duplex[1] and $\eta = 2$ for the half-duplex.

[1]For simplicity, we assumed that the loop interference is negligible at the relay

Since the MMSE receiver $\mathbf{L}$ at the relay is information lossless, it is immediate that setting $\mathbf{Q} = \mathbf{B}\mathbf{L}$ incurs no optimality loss in terms of the MIR criterion. For a given $\mathbf{Q} = \mathbf{B}\mathbf{L}$, the end-to-end mutual information (MI) in (16) is equivalently unfolded by

$$\begin{aligned}
\mathcal{I}(\mathbf{Q}) &= \frac{1}{\eta}\log|\rho\mathbf{I}_{N_S}|\left|\mathbf{R}_e^{-1}(\mathbf{B})\right|\\
&= \frac{1}{\eta}\log|\rho\mathbf{I}_{N_S}| - \frac{1}{\eta}\log\big|(\mathbf{H}^H\mathbf{H} + \rho^{-1}\mathbf{I}_{N_S})^{-1}\\
&\quad + \widetilde{\mathbf{U}}_h\big(\widetilde{\mathbf{U}}_h^H\mathbf{B}^H\mathbf{G}^H\mathbf{G}\mathbf{B}\widetilde{\mathbf{U}}_h + \widetilde{\mathbf{\Lambda}}_y^{-1}\big)^{-1}\widetilde{\mathbf{U}}_h^H\big|\\
&= \frac{1}{\eta}\log\left|\rho\mathbf{H}^H\mathbf{H} + \mathbf{I}_{N_S}\right| - \frac{1}{\eta}\log\big|(\widetilde{\mathbf{\Lambda}}_h + \rho^{-1}\mathbf{I}_M)\\
&\quad \times\big(\widetilde{\mathbf{U}}_h^H\mathbf{B}^H\mathbf{G}^H\mathbf{G}\mathbf{B}\widetilde{\mathbf{U}}_h + \widetilde{\mathbf{\Lambda}}_y^{-1}\big)^{-1}\big|, \qquad (17)
\end{aligned}$$

where the relay precoder $\mathbf{B}$ must be chosen to fulfil the relay power constraint $\text{Tr}(\mathbf{B}\mathbf{R}_y\mathbf{B}^H) \leq P_R$.

Let $\mathbf{\Phi} \in \mathbb{C}^{M\times M}$ be an arbitrary diagonal matrix. Then, similar to the MMSE solution in Section III-A, one can show that the optimal relay precoder which maximizes the MI in (17) is given by $\mathbf{B} = \widetilde{\mathbf{U}}_g\mathbf{\Phi}\mathbf{\Lambda}_y^{-1/2}\widetilde{\mathbf{U}}_h^H$. Substituting the result back into (17), the original MIR problem now reduces to a simple convex problem with respect to $|\mathbf{\Phi}|^2$ as

$$\begin{aligned}
\max_{|\mathbf{\Phi}|^2} \; & \mathcal{I}(\mathbf{\Phi}) = -\frac{1}{\eta}\log\left|\mathbf{I}_M + \rho\widetilde{\mathbf{\Lambda}}_h\big(\widetilde{\mathbf{\Lambda}}_g|\mathbf{\Phi}|^2 + \mathbf{I}_M\big)^{-1}\right|\\
s.t. \; & \text{Tr}(|\mathbf{\Phi}|^2) \leq P_R. \qquad (18)
\end{aligned}$$

The solution is readily found using a Lagrangian multiplier μ as $\mathbf{Q} = \widetilde{\mathbf{U}}_g\mathbf{\Phi}\widetilde{\mathbf{\Lambda}}_y^{-1/2}\widetilde{\mathbf{U}}_h^H\mathbf{L}$ where the i-th diagonal element of $\mathbf{\Phi}$, namely, ϕ_i is obtained from $|\phi_i|^2 = \frac{1}{2\lambda_{g,i}}\left[\sqrt{4\rho\lambda_{h,i}\lambda_{g,i}\mu + \rho^2\lambda_{h,i}^2} - \rho\lambda_{h,i} - 2\right]$ with μ being chosen to satisfy $\text{Tr}(|\mathbf{\Phi}|^2) \leq P_R$.

D. Naive Schemes

When no CSI is available at the relay, a sensible transmission strategy is isotropic [17] [14], i.e., $\hat{\mathbf{Q}} = \delta\mathbf{I}_{N_R}$, which is called *"Naive-MMSE"* or *"Naive-ZF"* depending on the equalizer used at the destination. The relay may use a scalar gain δ such that $\delta \leq \sqrt{\frac{P_R}{E[\mathbf{y}_R\mathbf{y}_R^H]}}$ to remain within the power constraint. However, this variable gain requires at least a long term estimation of the source-to-relay channel. Alternatively, we can exploit a fixed gain relay which amplifies the received signal with a constant factor c, i.e., $\delta = c$ [28]. Note that both cases exhibit the same diversity behavior as will be clear in the subsequent section.

IV. Diversity-Multiplexing Tradeoff Analysis

The DMT analysis provides a compact characterization of the tradeoff between the data rate and block-error probability over the MIMO quasi-static fading channels. For this reason, the DMT has been widely exploited as a convenient tool for comparing various relaying systems with different protocols. In this section, our goal is to identify the DMT performance of several linear transceiving schemes which have been most commonly adopted in AF relaying systems such as the naive, ZF, MMSE, and MIR designs.

Throughout the analysis, we say that a system achieves multiplexing gain r and corresponding diversity gain $d(r)$ if

$$\lim_{\rho\to\infty}\frac{R(\rho)}{\log\rho}\doteq r,\quad\text{and}\quad \lim_{\rho\to\infty}\frac{P_{\text{out}}(\rho)}{\log\rho}\doteq d(r),$$

where $R(\rho)$ denotes a certain target data rate that varies depending on the input SNR ρ and P_{out} indicates the outage probability. Therefore, $d(r)$ represents the DMT function. Note that if the rate $R(\rho)$ is a fixed constant for all SNRs, the multiplexing gain is zero by definition. In this case, the DRT function, i.e., $d(R)$ will replace the DMT. We assume the infinite length Gaussian codewords so that the error event is dominated by the outage event of MI[2]. For simplicity, we consider equal power cases, i.e., $P_R = P_T = \rho N_t$, but the result can be extended to more general cases. We use $N_S\times N_R\times N_D$ to denote a relaying system with N_S-source, N_R-relay, and N_D-destination antennas.

The optimal DMT $d^*(r)$ represents the best possible error probability exponent achievable over a channel by any space-time codes at a multiplexing gain r. Before we proceed with our analysis, we first establish the optimal DMT of the MIMO AF relay channel. This can be done by analyzing the DMT performance of the MIR design in Section III-C.

Theorem 1: The MIR transceiver achieves the optimal DMT of MIMO AF relaying systems which is given by

$$d^*(r) = (N_R-\eta r)(\min(N_S,N_D)-\eta r), \tag{19}$$

where $\eta = 1$ and 2 for the full-duplex and half-duplex relay, respectively, and $0<r<\frac{N}{\eta}$ with $N\triangleq\min(N_S,N_R,N_D)$.

Proof: The converse proof is immediate from the cut-set bound [17], because the end-to-end DMT of a relaying system is bounded by the DMT of the source-to-relay cut and the relay-to-destination cut, each of which is a P2P MIMO channel. As the transmission occurs over η-time phases, we obtain $d^*(r)$ in (19) by simply scaling the multiplexing gain γ by η. The remaining proof is to show that the MIR transceiver in III-C actually achieves the cut-set bound. Details are given in Appendix A. ■

While $d^*(r)$ is achievable by the ML decoding at the destination, the following result characterizes the DMT of MIMO AF relaying channels under the linear receivers. With the linear ZF or MMSE equalizer at the destination, the outage performance is characterized by the following two probabilities. As for the joint encoding scheme, the outage probability of interest is given by

$$P_{\text{out}}^{\text{JE}}\triangleq P\left(\frac{1}{\eta}\sum_{i=1}^{N_S}\log(1+\tau_i)<R(\rho)\right), \tag{20}$$

where τ_i indicates the output SNR of the i-th data stream. Meanwhile, for the separate encoding scheme, a reasonable strategy without CSI at the source is to allocate the same rate R/N_S to each stream. Then, the relevant outage probability is given by

$$P_{\text{out}}^{\text{SE}}\triangleq P\left(\bigcup_{i=1}^{N_S}\left\{\frac{1}{\eta}\log(1+\tau_i)<\frac{R(\rho)}{N_S}\right\}\right). \tag{21}$$

[2]The practical finite-length code design whose diversity order approaches the outage exponent is under investigation for our future works

Using these outage definitions, we characterize the DMT performance of the MMSE transceiver as a closed-form expression in the following theorem.

Theorem 2: The DMT of the $N_S\times N_R\times N_D$ MIMO AF relaying channels with the MMSE transceiver is given by

$$d_{ME}(r) = \begin{cases}(N_R-N_S+1)\left(1-\frac{\eta r}{N_S}\right)^+ & \text{if } N_S\le\min(N_R,N_D)\\ 0 & \text{otherwise}\end{cases} \tag{22}$$

for both the joint and separate encoding schemes with multiplexing gain $r>0$.

Proof: As it is clear from (20) and (21) that $P_{\text{out}}^{\text{JE}}\le P_{\text{out}}^{\text{SE}}$ for any linear transceivers $\mathbf{Q}$ and $\mathbf{W}$, we prove the theorem by showing that the upper-bound of $P_{\text{out}}^{\text{SE}}$ yields the same outage exponent as the lower-bound of $P_{\text{out}}^{\text{JE}}$. Note that with the MMSE strategy, the k-th output SNR equals $\tau_k=\rho/[\mathbf{R}_e]_{k,k}-1$ [26] and the target rate R is set to be $R(\rho)=r\log\rho$ with $r>0$.

(1) DMT Lower-bound: When the separate encoding is concerned with the MMSE transceiver, the outage probability (21) is equivalently

$$P_{\text{out}}^{\text{SE}} \;\doteq\; \max_i P\left(\frac{1}{\eta}\log\left(\frac{\rho}{[\mathbf{R}_e]_{i,i}}\right)<\frac{R(\rho)}{N_S}\right). \tag{23}$$

Then, applying $\hat{\mathbf{B}}$ described in (11) to the error covariance matrix (8), we obtain

$$P_{\text{out}}^{\text{SE}} \;\doteq\; P\Big(-\log\big(\min_i(S_{h,i}+S_{g,i})\big)<\frac{\eta R(\rho)}{N_S}\Big), \tag{24}$$

where

$$\begin{aligned}S_{h,i} &\triangleq [\mathbf{U}_h(\rho\mathbf{\Lambda}_h+\mathbf{I}_{N_S})^{-1}\mathbf{U}_h^H]_{i,i}\\ &= \mathbf{u}_i(\rho\mathbf{\Lambda}_h+\mathbf{I}_{N_S})^{-1}\mathbf{u}_i^H\\ &= \sum_{k=1}^{N_S}\frac{|u_{k,i}|^2}{1+\rho\lambda_{h,k}}\end{aligned} \tag{25}$$

with $\mathbf{u}_i$ being the i-th row of the unitary matrix $\mathbf{U}_h$ and $u_{k,i}$ being the k-th element of this column. Similarly, we obtain

$$\begin{aligned}S_{g,i} &\triangleq \widetilde{\mathbf{U}}_h(\rho\hat{\mathbf{\Phi}}\widetilde{\mathbf{\Lambda}}_g\hat{\mathbf{\Phi}}+\rho\widetilde{\mathbf{\Lambda}}_y)^{-1}\widetilde{\mathbf{U}}_h^H]_{i,i}\\ &= \sum_{k=1}^{M}\frac{|u_{k,i}|^2}{|\hat{\phi}_k|^2\rho\lambda_{g,k}+\rho\lambda_{y,k}^{-1}}.\end{aligned} \tag{26}$$

As it is always true that $|u_{k,i}|^2\le 1$ for all (k,i), it simply follows from (24) that

$$\begin{aligned}&P_{\text{out}}^{\text{SE}}\\ &\dot{\le} P\Bigg(\sum_{k=1}^{N_S}\frac{1}{1+\rho\lambda_{h,k}}+\sum_{k=1}^{M}\frac{1}{|\hat{\phi}_k|^2\rho\lambda_{g,k}+\rho\lambda_{y,k}^{-1}}>2^{-\frac{\eta R(\rho)}{N_S}}\Bigg)\\ &\le P\Bigg(\sum_{k=1}^{N_S}\frac{1}{1+\rho\lambda_{h,k}}+\sum_{k=1}^{M}\frac{1}{\eta\rho\lambda_{g,k}+\rho\lambda_{y,k}^{-1}}>2^{-\frac{\eta R(\rho)}{N_S}}\Bigg),\end{aligned} \tag{27}$$

where the second inequality holds because $\hat{\mathbf{\Phi}}$ is optimum in terms of the trace minimization as shown in (10) and we have

$$\sum_{k=1}^{M}\frac{1}{|\hat{\phi}_k|^2\rho\lambda_{g,k}+\rho\lambda_{y,k}^{-1}}=\mathrm{Tr}\big(\rho\hat{\mathbf{\Phi}}^H\widetilde{\mathbf{\Lambda}}_g\hat{\mathbf{\Phi}}+\rho\widetilde{\mathbf{\Lambda}}_y^{-1}\big)^{-1}.$$

Thus, setting $\hat{\mathbf{\Phi}} = \sqrt{\eta}\mathbf{I}_M$ clearly leads to the outage upper-bound (27). In addition, the following lemma, proven in Appendix B, implies that $\text{Tr}(\mathbf{B}\mathbf{R}_y\mathbf{B}^H) < \text{Tr}(\rho\mathbf{B}\mathbf{B}^H) = \text{Tr}(\rho\hat{\mathbf{\Phi}}\hat{\mathbf{\Phi}}^H)$, which means that η can be chosen as 1 to satisfy the relay power constraint.

Lemma 3: The covariance matrix of the relay signal $\mathbf{y}$ *(or the MMSE estimate of* $\mathbf{x}$ *at the relay) in (6) is upper-bounded by the identity matrix as* $\mathbf{R}_y \preceq \rho\mathbf{I}_{N_S}$.

Using the results presented above and setting $R(\rho) = r\log\rho$, we obtain

$$P_{\text{out}}^{\text{SE}} \dot{\leq} P\Big(\sum_{k=1}^{N_S}\frac{1}{1+\rho\lambda_{h,k}} + \sum_{k=1}^{M}\frac{1}{\rho\lambda_{g,k}+\rho\lambda_{y,k}^{-1}} > \rho^{-\frac{\eta r}{N_S}}\Big) \quad (28)$$

$$\leq P\Big(\frac{1}{\rho\lambda_{h,N_S}} + \frac{1}{\rho\lambda_{g,M}} > \rho^{-\frac{\eta r}{N_S}}\Big), \quad (29)$$

Finally, applying the harmonic mean bounds, i.e., $\frac{\min(a,b)}{2} \leq \frac{ab}{a+b} \leq \min(a,b)$ for $a > 0$ and $b > 0$, we have the trivial asymptotic upper-bound

$$P_{\text{out}}^{\text{SE}} \dot{\leq} P\left(\mu < \rho^{-\left(1-\frac{\eta r}{N_S}\right)}\right) \quad (30)$$

with $\mu \triangleq \min(\lambda_{h,N_S}, \lambda_{g,M})$. We notice that the upper-bound (30) vanishes only when $\eta r/N_S < 1$. Hence, the outage exponent lower-bound equals zero for $\eta r/N_S \geq 1$. Supposing $\eta r/N_S < 1$, we can write $P_{\text{out}} \dot{\leq} F_\mu\big(\rho^{-(1-\frac{\eta r}{N_S})^+}\big)$ where $F_\mu(\cdot)$ stands for the cumulative distribution function of μ.

Meanwhile, the result in [29, Lemma 2] implies that for a small argument $\delta \ll 1$, $F_\mu(\delta)$ asymptotically equals

$$F_\mu(\delta) \doteq F_{\lambda_{h,N_S}}(\delta) + F_{\lambda_{g,M}}(\delta) \quad (31)$$

where $F_{\lambda_{h,N_S}}(\delta) \propto \delta^{(N_R-N_S+1)^+}$ and $F_{\lambda_{g,M}}(\delta) \propto \delta^{(N_R-M+1)(N_D-M+1)^+}$ [30]. Therefore, the resulting outage upper-bound is

$$\begin{aligned} P_{\text{out}}^{\text{SE}} &\dot{\leq} \rho^{(N_R-N_S+1)^+\min(1,(N_D-M+1)^+)\left(1-\frac{\eta r}{N_S}\right)^+} \\ &= \rho^{-d_{\text{ME}}(r)}, \end{aligned} \quad (32)$$

and we establish the DMT lower-bound of the sperate encoding scheme.

(2) DMT Upper-bound : In what follows, we examine the DMT upper-bound of the joint encoding scheme. As $\log(\cdot)$ is a concave function, $P_{\text{out}}^{\text{JE}}$ in (20) is bounded by the Jensen's inequality as

$$\begin{aligned} P_{\text{out}}^{\text{JE}} &\geq P\left(\frac{N_S}{\eta}\log\left(\frac{1}{N_S}\sum_{i=1}^{N_S}\frac{\rho}{[\mathbf{R}_e]_{i,i}}\right) < R(\rho)\right) \\ &= P\left(\frac{1}{N_S}\sum_{i=1}^{N_S}\frac{1}{S_{h,i}+S_{g,i}} < \rho^{\frac{\eta r}{N_S}}\right) \\ &\geq P\left(\min_i(S_{h,i}+S_{g,i}) > \rho^{-\frac{\eta r}{N_S}}\right), \end{aligned} \quad (33)$$

where $S_{h,i}$ and $S_{g,i}$ are defined in (25) and (26), respectively.

Now, let us define $\bar{i} \triangleq \arg\min_i S_{h,i} + S_{g,i}$ and let $\mathcal{A}$ be the event $\{|u_{k,\bar{i}}|^2 \geq \frac{1-\epsilon}{N_S},\ \forall k\}$ where $\epsilon > 0$ is a small positive number independent of ρ. Then, we can show that $P(\mathcal{A})$ is finite and independent of ρ, i.e, $P(\mathcal{A}) \doteq \rho^0$ similar to [31, Appendix A]. Therefore, the outage probability can be further bounded by

$$\begin{aligned} P_{\text{out}}^{\text{JE}} &\geq P\Big(\sum_{k=1}^{N_S}\frac{|u_{k,\bar{i}}|^2}{1+\rho\lambda_{h,k}} \\ &\qquad + \sum_{k=1}^{M}\frac{|u_{k,\bar{i}}|^2}{|\hat{\phi}_k|^2\rho\lambda_{g,k}+\rho\lambda_{y,k}^{-1}} > \rho^{-\frac{\eta r}{N_S}}\Big|\mathcal{A}\Big)P(\mathcal{A}) \\ &\dot{\geq} P\Big(\sum_{k=1}^{N_S}\frac{1}{1+\rho\lambda_{h,k}} \\ &\qquad + \sum_{k=1}^{M}\frac{1}{|\hat{\phi}_k|^2\rho\lambda_{g,k}+\rho\lambda_{y,k}^{-1}} > \frac{N_S}{1-\epsilon}\rho^{-\frac{\eta r}{N_S}}\Big) \\ &\geq P\Big(\sum_{k=1}^{N_S}\frac{1}{1+\rho\lambda_{h,k}} \\ &\qquad + \sum_{k=1}^{M}\frac{1}{N_S\rho\lambda_{y,k}^{-1}(1+\rho\lambda_{g,k})} > \frac{N_S}{1-\epsilon}\rho^{-\frac{\eta r}{N_S}}\Big), \end{aligned} \quad (34)$$

where the last inequality holds from the constraint $\text{Tr}(\mathbf{B}\mathbf{R}_y\mathbf{B}^H) \leq N_S\rho$ which implies that $\hat{\mathbf{\Phi}}\widetilde{\mathbf{\Lambda}}_y\hat{\mathbf{\Phi}}^H \preceq \rho N_S\mathbf{I}_M$; thus, $|\hat{\phi}_k|^2 \leq N_S\rho\lambda_{y,k}^{-1}$ for all $k = 1,\ldots,M$. Note that from the definition of $\mathbf{R}_y$ (see (59) in Appendix B), we have $\rho\lambda_{y,k}^{-1} = 1 + \rho^{-1}\lambda_{h,k}^{-1}$ for all k. Recalling that the multiplexing gain $r > 0$ is assumed to be positive, the right-hand side of (34) vanishes, and thus the scaling factor $N_S/(1-\epsilon)$ does not affect the diversity order. In other words, the outage lower-bound is equivalently

$$\begin{aligned} P_{\text{out}}^{\text{JE}} \dot{\geq} P\Big(&\frac{1}{1+\rho\lambda_{h,N_S}} \\ &+ \frac{1}{(1+\rho^{-1}\lambda_{h,M}^{-1})(1+\rho\lambda_{g,M})} > \rho^{-\frac{\eta r}{N_S}}\Big). \end{aligned} \quad (35)$$

Now, let us define

$$\alpha_i \triangleq -\frac{\log\lambda_{h,i}}{\log\rho} \quad \text{and} \quad \beta_j \triangleq -\frac{\log\lambda_{g,j}}{\log\rho}, \quad (36)$$

for $i = 1,\ldots,N_S$ and $j = 1,\ldots,M$. In addition, we define a positive real number $0 < \kappa < 1$ as $\kappa \triangleq 1 - 2r/N_S$ to make the outage expression more compact. Then, (35) is alternatively expressed as

$$\begin{aligned} P_{\text{out}}^{\text{JE}} &\dot{\geq} P\Big(\frac{1}{1+\rho^{1-\alpha_{N_S}}} \\ &\qquad + \frac{1}{(1+\rho^{-(1-\alpha_{N_S})})(1+\rho^{1-\beta_M})} > \rho^{-\frac{\eta r}{N_S}}\Big) \\ &\doteq P\Big(\frac{1}{\rho^{\kappa-\alpha_{N_S}}} \\ &\qquad + \frac{1}{\rho^{\alpha_{N_S}-(2-\kappa)} + \rho^{\kappa-\beta_M} + \rho^{\kappa-\beta_M+\alpha_{N_S}-1}} > 1\Big) \\ &\doteq P\Big(\frac{1}{\rho^{\kappa-\alpha_M}} + \frac{1}{\rho^{\alpha_{N_S}-(2-\kappa)} + \rho^{\max(\kappa,\kappa+\alpha_{N_S}-1)-\beta_M}} \\ &\qquad > 1\Big|\alpha_{N_S} > \kappa\Big)P\big(\alpha_{N_S} > \kappa\big) \\ &= P\Big(\frac{1}{\rho^{\kappa-\alpha_{N_S}}} + \frac{1}{\rho^{\alpha_{N_S}-(2-\kappa)} + \rho^{\max(\kappa,\kappa+\alpha_{N_S}-1)-\beta_M}} \\ &\qquad > 1\Big|\alpha_{N_S} < \kappa\Big)P\big(\alpha_{N_S} < \kappa\big) \end{aligned}$$

$$\stackrel{(a)}{\doteq} P\left(\alpha_{N_S} > \kappa\right) + P\left(\beta_M > \kappa\right) P\left(\alpha_{N_S} < \kappa\right)$$
$$\stackrel{(b)}{\doteq} F_{\lambda_{h,N_S}}(\rho^{-\kappa}) + F_{\lambda_{g,M}}(\rho^{-\kappa}), \quad (37)$$

where (a) is due to the following exponential equalities:

$$\frac{1}{\rho^{\kappa-\alpha_{N_S}}} \doteq \begin{cases} \infty & \text{if } \alpha_{N_S} > \kappa \\ 0 & \text{if } \alpha_{N_S} < \kappa \end{cases}$$

$$\frac{1}{\rho^{\alpha_{N_S}-(2-\kappa)} + \rho^{\max(\kappa,\kappa+\alpha_{N_S}-1)-\beta_M}}$$
$$\doteq \begin{cases} \infty & \text{if } \alpha_{N_S} < 2-\kappa \text{ and } \beta_M > \max(\kappa,\kappa+\alpha_{N_S}-1) \\ 0 & \text{if } \alpha_{N_S} > 2-\kappa \text{ or } \beta_M < \max(\kappa,\kappa+\alpha_{N_S}-1) \end{cases}$$

and (b) follows from the fact that $P(\alpha_k < \kappa) \doteq \rho^0$ for any k [12]. Note that since $\lambda_{h,k}$ and $\lambda_{g,k}$ are continuous random variables on the positive real domain, the probability of α_k or β_k taking any value on the discontinuity point, e.g., $\alpha_{N_S} = \kappa$, is negligible [31]. Now, it is immediate to check that (37) is asymptotically equivalent to (30). Therefore, applying the same argument as in (31), we find out that the DMT upper-bound coincides with the previously found lower-bound, and the proof is concluded. ■

Compared to the MIR design enjoying the optimal DMT in (19), Theorem 2 demonstrates that the MMSE transceiver suffers from a diversity loss. This is due to the fact that the linear MMSE equalizer at the destination enforces the transmitted symbols to be spatially separated at the destination at the cost of the diversity order. It is also observed that with the MMSE criterion, there may be no advantage in coding across antennas in terms of the DMT compared to the separate encoding scheme. This is because the output SNRs of virtual parallel channels, i.e., τ_k's become strongly correlated with each other, and thus only the minimum eigenvalue in each hop essentially dominates the performance as in (35).

The DMT expression in (22) shows that the antenna configuration in the second-hop link does not affect the diversity order of MIMO AF relaying systems as long as $N_S \le N_D$. Thus, a use of multiple antennas at the destination greater than N_S may not be advantageous in terms of the DMT. It is also of interest to compare the MMSE transceiver in $N_S \times N_R \times N_D$ relay channels with the MMSE receiver in $N_S \times N_D$ P2P channels [31, Theorem 1]. It is immediate to check that if we deploy a relay node between the transmitter and the receiver such that $N_R > N_D$, a higher diversity gain as well as the coverage extension can be achieved over the P2P channels. although the multiplexing gain will be cut in half when the half-duplex relay is adopted.

It is also important to remark that Theorem 2 is valid only for the positive multiplexing gain $r > 0$. This is due to the limitation of the DMT framework which do not distinguish between different spectral efficiencies having the same multiplexing gain. In fact, if $r = 0$, the bound in (35), which is connected to the DMT upper-bound of the joint encoding scheme, does not hold in general because each summation term in (34) is bounded above as $1/(1+\rho\lambda_{h,k}) < 1$ and $1/(\rho\lambda_{y,k}^{-1}(1+\rho\lambda_{g,k})) < 1$ for all k. Accordingly, for a small transmit rate R, the outage event may occur when other eigenvalues which do not appear in (35) play a role, which typically leads to a higher diversity gain than (22). Indeed, the MMSE transceiver exhibits ML-like performance in cases where the coding is applied across antennas with sufficiently low spectral efficiency. Details will be addressed in Section V through the DRT analysis.

In the meantime, the ZF transceiver obtains the same DMT as one in (22) as shown in the following theorem, and thus our statement so far is also applicable to the ZF transceiver. However, it is worthwhile noting that unlike the MMSE transceiver in Theorem 2, the DMT with the ZF transceiver holds for every multiplexing gain $r \ge 0$. Therefore, the joint and separate coding schemes yield completely the same diversity order.

Theorem 3: In $N_S \times N_R \times N_d$ MIMO AF relaying channels, the DMT of the ZF transceiver is the same as $d_{ME}(r)$ in (22) for both the joint and separate encoding schemes and holds for all multiplexing gain $r \ge 0$.

Proof: Similar to Theorem 2, the proof can be made by showing that the upper-bound of $P_{\text{out}}^{\text{JE}}$ and the lower-bound of $P_{\text{out}}^{\text{JE}}$ are asymptotically equivalent. With the ZF strategy, we notice that $N_S \le \min(N_R, N_D)$ and $\tau_k = \rho/[\mathbf{R}_e]_{k,k}$ [26], and set the target data rate by $R(\rho) = r\log\rho$ with $r \ge 0$. The following lemma, proven in Appendix C, will be useful during our derivations.

Lemma 4: The covariance matrix of the relay signal $\mathbf{z}$ (or the ZF estimate of $\mathbf{x}$ at the relay) in (15) is exponentially equivalent to the identity matrix as $\mathbf{R}_z \doteq \rho\mathbf{I}_{N_S}$.

(1) DMT Lower-bound: From the results in Section III-B and (21), the outage probability, constrained to use the separate encoding, is written by

$$P_{\text{out}}^{\text{SE}} \doteq \max_i P\Bigg(\log\Bigg(1 + \frac{\rho}{\left[(\mathbf{H}^H\mathbf{H})^{-1}\right]_{i,i} + \left[(\mathbf{U}_h\hat{\mathbf{\Phi}}\widetilde{\mathbf{\Lambda}}_g\hat{\mathbf{\Phi}}^H\mathbf{U}_h^H)^{-1}\right]_{i,i}}\Bigg) < \frac{\eta R(\rho)}{N_S}\Bigg)$$
$$\le P\Bigg(\min_i\Big(\left[(\rho\mathbf{H}^H\mathbf{H})^{-1}\right]_{i,i} + \left[(\rho\mathbf{U}_h\hat{\mathbf{\Phi}}\widetilde{\mathbf{\Lambda}}_g\hat{\mathbf{\Phi}}^H\mathbf{U}_h^H)^{-1}\right]_{i,i}\Big) > \rho^{-\frac{\eta r}{N_S}}\Bigg)$$
$$\le P\left(\text{Tr}\big((\rho\mathbf{H}^H\mathbf{H})^{-1}\big) + \text{Tr}\big((\rho\hat{\mathbf{\Phi}}\widetilde{\mathbf{\Lambda}}_g\hat{\mathbf{\Phi}}^H)^{-1}\big) > \rho^{-\frac{\eta r}{N_S}}\right).$$

Meanwhile, it is revealed from Lemma 4 that $\text{Tr}(\mathbf{B}\mathbf{R}_z\mathbf{B}^H) \doteq \text{Tr}(\rho\hat{\mathbf{\Phi}}\hat{\mathbf{\Phi}}^H) \le N_S\rho$. Therefore, by setting $\hat{\mathbf{\Phi}} = \mathbf{I}_{N_S}$, the outage probability can be further bounded by

$$P_{\text{out}}^{\text{SE}} \ \dot{\le}\ P\left(\sum_{i=1}^{N_S}\frac{1}{\rho\lambda_{h,i}} + \sum_{i=1}^{N_S}\frac{1}{\rho\lambda_{g,i}} > \rho^{-\frac{\eta r}{N_S}}\right)$$
$$\doteq P\left(\frac{1}{\rho\lambda_{h,N_S}} + \frac{1}{\rho\lambda_{g,N_S}} > \rho^{-\frac{\eta r}{N_S}}\right),$$

which is equivalent to the previous result in (29), and thus the DMT lower-bound is established.

(2) DMT Upper-bound: Considering the output SNR of the ZF transceiver and applying the Jensen's inequality, the outage probability (20) is lower-bounded by

$$\begin{aligned} P_{\text{out}}^{\text{JE}} &\geq P\Big(\frac{N_S}{2}\log\Big(\frac{1}{N_S}\sum_{k=1}^{N_S}\big(1+\frac{\rho}{[\mathbf{R}_e]_{k,k}}\big)\Big) < R(\rho)\Big) \\ &\dot{\geq} P\Big(\min_i\big([(\rho\mathbf{U}_h\mathbf{\Lambda}_h\mathbf{U}_h^H)^{-1}]_{i,i} \\ &\quad + \big[(\rho\mathbf{U}_h\hat{\mathbf{\Phi}}\widetilde{\mathbf{\Lambda}}_g\hat{\mathbf{\Phi}}^H\mathbf{U}_h^H)^{-1}\big]_{i,i}\big) > \rho^{-\frac{\eta r}{N_S}}\Big). \end{aligned}$$

According to Lemma 4, the relay power constraint is asymptotically $\text{Tr}(\rho\hat{\mathbf{\Phi}}\hat{\mathbf{\Phi}}^H) \leq N_S\rho$; thus, we have $\hat{\mathbf{\Phi}}\hat{\mathbf{\Phi}}^H \preceq N_S\mathbf{I}_{N_S}$, i.e., $|\hat{\phi}_k|^2 \leq N_S$ for all k. Then, applying the same argument as in (34), we obtain

$$\begin{aligned} &P_{\text{out}}^{\text{JE}} \\ &\dot{\geq} P\Big(\min_i\Big(\sum_{k=1}^{N_S}\frac{|u_{k,i}|^2}{\rho\lambda_{h,k}} + \sum_{k=1}^{N_S}\frac{|u_{k,i}|^2}{|\hat{\phi}_k|^2\rho\lambda_{g,k}}\Big) > \rho^{-\frac{\eta r}{N_S}}\Big) \\ &\doteq P\left(\sum_{k=1}^{N_S}\frac{1}{\rho\lambda_{h,k}} + \sum_{k=1}^{N_S}\frac{1}{N_S\rho\lambda_{g,k}} > \frac{N_S}{1-\epsilon}\rho^{-\frac{\eta r}{N_S}}\right) \quad (38) \\ &\doteq P\left(\frac{1}{\rho\lambda_{h,N_S}} + \frac{1}{\rho\lambda_{g,N_S}} > \rho^{-\frac{\eta r}{N_S}}\right), \quad (39) \end{aligned}$$

which exhibits the same outage expression as (29); thus, the DMT upper-bound is readily obtained by following similar steps from (30) to (32). We note that in contrast to the previous result in (34), each summation term in (38) is unbounded above for small channel gains $\rho\lambda_{h,k}$ or $\rho\lambda_{g,k}$, which implies that there is no room for the eigenvalues larger than λ_{h,N_S} and λ_{g,N_S} to contribute to the outage probability in (38) no matter which coding scheme is applied with finite rate ($r = 0$). Therefore, the derived DMT holds for all multiplexing gain $r \geq 0$. ■

In what follows, we study the DMT performance of the naive-ZF and -MMSE schemes to examine the effect of no CSI at the relay.

Theorem 4: The DMT of the $N_S \times N_R \times N_d$ MIMO AF relaying channels with the naive-MMSE is given by

$$d_{\text{N-ME}}(r) = (\min(N_R, N_D) - N_S + 1)^+\left(1 - \frac{\eta r}{N_S}\right)^+ \quad (40)$$

for both the joint and separate encoding schemes with positive multiplexing gain $r > 0$.

Proof: Let us assume that $\mathbf{Q} = \delta\mathbf{I}_{N_R}$ where δ is chosen to satisfy the relay power constraint (7) as

$$\delta^2 = \frac{P_R}{\text{Tr}(\rho\mathbf{H}\mathbf{H}^H + \mathbf{I}_{N_R})} = \left(\frac{1}{N_S}\sum_{k=1}^{N_S}\lambda_{h,k} + \rho^{-1}\right)^{-1}. \quad (41)$$

Then, it is readily seen that $\delta \doteq c$ for some real positive value c because we have $\frac{1}{N_S}\sum_{k=1}^{N_S}\rho^{-\alpha_k} \doteq \rho^0$, i.e., the variable gain δ based on the channel state $\mathbf{H}$ is exponentially equivalent to the fixed gain relay $\delta = c$. Similarly, one can show that $\mathbf{I}_{N_D} \succeq \mathbf{R}_n^{-1} \succeq (1 + \delta^2\lambda_{g,1})^{-1}\mathbf{I}_{N_D} \doteq \rho^0\mathbf{I}_{N_D}$ [14], which means that the amplified noise at the relay does not affect the diversity order; thus, the naive relaying can be regarded as a Rayleigh product channel [20] whose error covariance matrix is given by $\mathbf{R}_e = (c\mathbf{H}^H\mathbf{G}^H\mathbf{G}\mathbf{H} + \rho^{-1}\mathbf{I}_{N_S})^{-1}$.

Keeping this in mind, let us focus on the outage lower-bound of the joint encoding scheme. Define $\lambda_{t,1} > \cdots > \lambda_{t,N_S}$ as the eigenvalues of $\mathbf{H}^H\mathbf{G}^H\mathbf{G}\mathbf{H}$. Then, setting the target rate $R(\rho) = r\log\rho$ with $r > 0$ and following the approaches as in (33) and (34), it is easy to show that

$$\begin{aligned} P_{\text{out}}^{\text{JE}} &\dot{\geq} P\left(\sum_{k=1}^{N_S}\frac{1}{1+\rho\lambda_{t,k}} > \frac{N_S}{1-\epsilon}\rho^{-\frac{\eta r}{N_S}}\right) \\ &\doteq P\left(\frac{1}{\rho\lambda_{t,N_S}} > \rho^{-\frac{\eta r}{N_S}}\right). \quad (42) \end{aligned}$$

First, we observe that if $N_S > \min(N_R, N_D)$, the outage probability (42) leads to a trivial solution $P_{\text{out}}^{\text{JE}} \dot{\leq} \rho^0$, due to the rank constraint of $\mathbf{H}^H\mathbf{G}^H\mathbf{G}\mathbf{H}$ which is equal to $N = \min(N_S, N_R, N_D)$. Thus, we assume $N_S \leq \min(N_R, N_D)$ from now on. Note that the exponential equality (42) holds only when $r > 0$ for similar reason to (35). Now, we define $\gamma_k \triangleq -\log\lambda_{t,k}/\log\rho$ for $k = 1, \ldots, N_S$. Then, (42) is further simplified as $P_{\text{out}}^{\text{JE}} \dot{\geq} P(\mathcal{E}_\gamma) \doteq \rho^{-d(r)}$ with the outage event $\mathcal{E}_\gamma \triangleq \{\gamma_{N_S} > (1 - \frac{\eta r}{N_S})^+\}$.

Let $f(\mathbf{c})$ be the p.d.f. of a random vector $\mathbf{c} = [\gamma_1, \ldots, \gamma_{N_S}]$ and $\theta(\mathbf{c})$ denote its exponential order, i.e., $f(\mathbf{c}) \doteq \rho^{-\theta(\mathbf{c})}$. Then, one can show that the DMT is calculated as [12]

$$d(r) = \inf_{\mathbf{c}\in\mathcal{E}_\gamma, \forall\gamma_k>0}\theta(\mathbf{c}).$$

For Rayleigh product channels, it was shown in [20] that $\theta(\mathbf{c})$ is given in three different forms according to antenna configurations[3], but we only need to consider two cases $N_R \leq N_D$ and $N_D < N_R$ since we assume $N_S = N$. For the first case, by applying the result (61) in Appendix D, we have

$$\begin{aligned} d(r) &\doteq \inf_{\mathbf{c}\in\mathcal{E}_\gamma, \forall\gamma_k>0}\theta_2(\mathbf{c}) \\ &= (N_R - N_S + 1)\left(1 - \frac{\eta r}{N_S}\right)^+, \end{aligned}$$

as the infimum is obtained when $\gamma_k = 0$ for $k = 1, \ldots, N_S - 1$ and $\gamma_{N_S} = 1$. Similarly, for the second case, by adopting the result in (62), we have

$$\begin{aligned} d(r) &\doteq \inf_{\mathbf{c}\in\mathcal{E}_\gamma, \forall\gamma_k>0}\theta_3(\mathbf{c}) \\ &= (N_D - N_S + 1)\left(1 - \frac{\eta r}{N_S}\right)^+. \end{aligned}$$

Finally, combining of the two, we prove that the DMT upper-bound equals $d_{\text{N-ME}}(r)$ in (40). Meanwhile, it is immediate to show that the separate encoding scheme achieves the same DMT. Details are trivial, and thus omitted. ■

On the other hand, with the naive-ZF, the error covariance matrix will be $\mathbf{R}_e = (c\mathbf{H}^H\mathbf{G}^H\mathbf{G}\mathbf{H})^{-1}$ which leads to the outage lower-bound

$$\begin{aligned} P_{\text{out}}^{\text{JE}} &\dot{\geq} P\left(\sum_{k=1}^{N_S}\frac{1}{\rho\lambda_{t,k}} > \frac{N_S}{1-\epsilon}\rho^{-\frac{\eta r}{N_S}}\right). \quad (43) \\ &\doteq P\left(\frac{1}{\rho\lambda_{t,N_S}} > \rho^{-\frac{\eta r}{N_S}}\right). \quad (44) \end{aligned}$$

[3] For completeness, some of key results of [20] are summarized in Appendix D.

Recall that each summation term $1/\rho\lambda_{t,k}$ in (43) is unbounded above for the small channel gain $\rho\lambda_{t,k}$. Therefore, in contrast to (42), the equality (44) holds for every multiplexing gain $r \geq 0$, from which the DMT of the naive-ZF follows.

Theorem 5: In the $N_S \times N_R \times N_d$ MIMO AF relaying channels, the DMT of the naive-ZF is the same as $d_{N\text{-}ME}(r)$ (40) for both the joint and separate encoding schemes and holds for all positive multiplexing gain $r \geq 0$.

The DMT analysis of the naive schemes provides useful insights on the AF relaying systems. First, it is seen from Theorem 4 and 5 that when the number of relay antennas is sufficiently small such that $N_R \leq N_D$, the naive schemes achieve the same DMT as the corresponding transceiving schemes studied in Theorem 2 and 3. In this case, therefore, knowing the CSI at the relay may not be significant.

However, as N_R grows larger than N_D, the naive schemes do not achieve proper diversity gains. This is because the transmit diversity is not fully exploited by the naive schemes due to the absence of the CSI at the relay.[4] Therefore, an intelligent relay matrix design based on the CSI is essential to obtain a proper diversity gain especially when $N_R > N_D$.

Similar to the MMSE transceiver, the DMT of the naive-MMSE only holds for positive multiplexing gain $r > 0$. In particular, when the rate is fixed and not too large, it is seen that very significant performance advantage is achieved by the joint encoding scheme. Unlike the MMSE transceiver, however, we should remark that the full-diversity order may not be achievable with the naive-MMSE scheme no matter how small the rate is. This statement will be demonstrated through the DRT analysis in the subsequent section.

V. Diversity-Rate Tradeoff Analysis with Joint Encoding

In this section, we aim to characterize the diversity order of the MMSE schemes as a function of the finite spectral efficiency R (b/s/Hz). The DMT analysis may be accurate for the positive multiplexing gain $r > 0$. However, when the rate is fixed and small, the MMSE schemes with the joint encoding at the source exhibits the performance in stark contrast to one predicted by the DMT. In particular, the MMSE transceiver even exhibits the full-diversity order when the rate is sufficiently low. In what follows, we characterize such an rate-dependent diversity behavior of the MMSE schemes through the DRT analysis and obtain tight upper and lower bounds of the diversity order as a function of target spectral efficiency R and the number of antennas at each node.[5]

Theorem 6: For a fixed spectral efficiency R, the DRT of the MMSE transceiver over $N_S \times N_R \times N_d$ MIMO AF relaying channels, constrained to use the joint encoding scheme, is given by

$$D_{ME}\left(\lceil (m)^+ \rceil\right) \leq d_{ME}(R) \leq D_{ME}\left(\lfloor (m+1)^+ \rfloor\right), \quad (45)$$

where $m \triangleq N_S 2^{-\frac{\eta R}{N_S}} + M - N_S$ and $D_{ME}(i) \triangleq \min\left(i(N_R + N_S - 2M + i), (N_R - M + i)(N_D - M + i)^+\right)$. The upper and lower bounds of (45) always meet except for some discontinuity points, i.e., $m = 1, 2, \ldots, N_s$.

Proof: **(1) DRT Lower-bound**: Consider the MMSE transceiver with the joint encoding scheme. Since $-\log(\cdot)$ is convex, applying the Jensen's inequality and setting the target rate as R, the outage probability of (20) is upper-bounded by

$$\begin{aligned} P_{\text{out}}^{\text{JE}} &\leq P\left(-\frac{N_S}{\eta}\log\left(\frac{1}{\rho N_S}\text{Tr}(\mathbf{R}_e)\right) < R\right) \quad (46) \\ &\leq P\Big(-\frac{N_S}{\eta}\log\Big(\frac{1}{N_S}\big(\text{Tr}(\rho\boldsymbol{\Lambda}_h + \mathbf{I}_{N_S})^{-1} \\ &\qquad + \text{Tr}\big(\rho\widetilde{\boldsymbol{\Lambda}}_g + \rho\widetilde{\boldsymbol{\Lambda}}_y^{-1}\big)^{-1}\big)\Big) < R\Big). \end{aligned}$$

Note that the last bound is obtained by setting $\hat{\boldsymbol{\Phi}} = \mathbf{I}_M$ as in (27). Then, by employing the definitions of α_k and β_k in (36), it follows

$$\begin{aligned} &P_{\text{out}}^{\text{JE}} \\ &\leq P\Big(\sum_{k=1}^{N_S}\frac{1}{1+\rho\lambda_{h,k}} + \sum_{k=1}^{M}\frac{1}{\rho\lambda_{g,k}+\rho\lambda_{y,k}^{-1}} > N_S 2^{-\frac{\eta R}{N_S}}\Big) \\ &= P\Big(\sum_{k=1}^{M}\frac{1}{1+\rho\lambda_{h,k}} + \sum_{k=1}^{M}\frac{1}{\rho\lambda_{g,k}+\rho\lambda_{y,k}^{-1}} \\ &\qquad\qquad > N_S 2^{-\frac{\eta R}{N_S}} + M - N_S\Big) \\ &\doteq P\Big(\sum_{k=1}^{M}\frac{1}{1+\rho^{1-\alpha_k}} \\ &\qquad + \sum_{k=1}^{M}\frac{1}{1+\rho^{1-\beta_k}+\rho^{-(1-\alpha_k)}} > (m)^+\Big), \quad (47) \end{aligned}$$

where (47) is due to the fact that the outage exponent will converge to 0 for all $m \leq 0$.

Asymptotically, the following exponential equalities hold:

$$\frac{1}{1+\rho^{1-\alpha_k}} \doteq \begin{cases} 1 & \text{if} \quad \alpha_k > 1 \\ 0 & \text{if} \quad \alpha_k < 1 \end{cases} \quad (48)$$

$$\frac{1}{1+\rho^{1-\beta_k}+\rho^{-(1-\alpha_k)}} \doteq \begin{cases} 1 & \text{if } \alpha_k < 1 \text{ and } \beta_k > 1 \\ 0 & \text{if } \alpha_k > 1 \text{ or } \beta_k < 1 \end{cases}, \quad (49)$$

for $k = 1, \ldots, M$, which implies that in order for the outage to occur, at least $\overline{m} \triangleq \lceil m^+ \rceil$ number of terms in (47) should be 1 among $2M$ summation terms. It is important to note that (48) and (49) cannot simultaneously be 1 at the same k, which is a key feature of the MMSE transceiver enabling us to achieve the full diversity order for sufficiently small rate R.

Recall that all eigenvalues are arranged in descending order, which means that $\{\alpha_i\}$ and $\{\beta_i\}$ are ordered according to $\alpha_1 \leq \cdots \leq \alpha_M$ and $\beta_1 \leq \cdots \leq \beta_M$. For example, if $\alpha_1 > 1$, the term in (49) converges to zero for all k, regardless of β. Using this property, we can define the event $\mathcal{X}_i$ in which the summation in the left-hand side of (47) equals i as

$$\mathcal{X}_i = \mathcal{E}_{h,i} \cup \mathcal{E}_{g,i,0} \cup \mathcal{E}_{g,i,1} \cup \cdots \cup \mathcal{E}_{g,i,i-1}$$

[4]It has been shown in [32] and [33] that the *"random sequential"* scheme may also improve the DMT performance of the naive scheme without needing to know the CSI at the relay. However, this scheme randomly changes the effective channel across the transmission block, which amounts to the time varying environment, and thus is beyond the scope of the paper.

[5]Note that tight bounds of the DRT with the separate encoding scheme are still open. However, extensive computer simulations demonstrate that the MMSE schemes with the separate encoding behaves as predicted by the DMT with $r = 0$ for entire range of R

for $i=1,\ldots,M$, where $\mathcal{E}_{h,i} \triangleq \{\alpha_{M-i+1} > 1 > \alpha_{M-i}\}$ and $\mathcal{E}_{g,i,j} \triangleq \{\beta_{M-i+1} > 1 > \beta_{M-i}\} \cap \mathcal{E}_{h,j}$ for $j=0,1,\ldots,i-1$. Then, from the union bound, we have

$$\begin{aligned} P_{\text{out}}^{\text{JE}} &\dot{\leq} P\left(\bigcup_{i=\overline{m}}^{M} \mathcal{X}_i\right) \\ &\leq \sum_{i=\overline{m}}^{M} \Big(P(\mathcal{E}_{h,i}) + \sum_{j=0}^{i-1} P(\mathcal{E}_{g,i,j})\Big), \end{aligned} \tag{50}$$

First, we define $P(\mathcal{E}_{h,i}) \doteq \rho^{-d_{h,i}(R)}$, $i=1,\ldots,M$. Then, applying Varadhan's lemma [31] [12] by using the asymptotic p.d.f.[6] of the random vector $\mathbf{a} = [\alpha_1,\ldots,\alpha_M]$ as

$$f(\mathbf{a}) \doteq \Big[\prod_{l=1}^{M} \rho^{-(N_S+N_R-2l+1)\alpha_l}\Big] \exp\Big(-\sum_{l=1}^{M} \rho^{-\alpha_l}\Big), \tag{51}$$

we obtain

$$\begin{aligned} d_{h,i}(R) &= \inf_{\mathbf{a}\in\mathcal{E}_{h,i},\forall\alpha_l>0} \sum_{l=1}^{M} (N_S+N_R-2l+1)\alpha_l \\ &= \sum_{l=1}^{M-i} (N_S+N_R-2l+1)\times 0 \\ &\quad + \sum_{l=M-i+1}^{M} (N_S+N_R-2l+1)\times 1 \\ &= i(N_R+N_S-2M+i). \end{aligned} \tag{52}$$

Now, let us examine the probability of the event $\mathcal{E}_{g,i,j}$, i.e., $P(\mathcal{E}_{g,i,j}) \doteq \rho^{-d_{g,i,j}(R)}$. Defining $L \triangleq \min(N_R, N_D)$, the p.d.f. of the random vector $\mathbf{b} = [\beta_1,\ldots,\beta_L]$ is given by

$$f(\mathbf{b}) \doteq \Big[\prod_{l=1}^{L} \rho^{-(N_R+N_D-2l+1)\beta_l}\Big] \exp\Big(-\sum_{l=1}^{L} \rho^{-\beta_l}\Big). \tag{53}$$

Then, the probability of the event $\mathcal{E}_{g,i,j}$ is

$$\begin{aligned} P(\mathcal{E}_{g,i,j}) &= \int_{\mathcal{E}_{g,i,j}} f(\mathbf{a},\mathbf{b}) d\mathbf{a} d\mathbf{b} \\ &\doteq \int_{\mathcal{E}_{g,i,j}} \Big[\rho^{-\sum_{l=1}^{M}(N_S+N_R-2l+1)\alpha_l - \sum_{l=1}^{L}(N_R+N_D-2l+1)\beta_l}\Big] \\ &\qquad \times \exp\Big(-\sum_{l=1}^{M}\rho^{-\alpha_l} - \sum_{l=1}^{L}\rho^{-\beta_l}\Big) d\mathbf{a} d\mathbf{b}, \end{aligned}$$

due to the independence of $\mathbf{a}$ and $\mathbf{b}$, and applying Varadhan's lemma again, we have

$$\begin{aligned} d_{g,i,j}(R) &= \inf_{(\mathbf{a},\mathbf{b})\in\mathcal{E}_{g,i,j},\forall\alpha_l,\forall\beta_l>0} \sum_{l=1}^{M}(N_S+N_R-2l+1)\alpha_l \\ &\quad + \sum_{l=1}^{L}(N_R+N_D-2l+1)\beta_l \\ &= \sum_{l=M-j+1}^{M} (N_S+N_R-2l+1) \\ &\quad + \sum_{l=M-i+1}^{L} (N_R+N_D-2l+1) \\ &= j(N_S+N_R-2M+j) \\ &\quad + (N_R+N_D-L-M+i)(L-M+i)^+ \\ &= j(N_S+N_R-2M+j) \\ &\quad + (N_R-M+i)(N_D-M+i)^+. \end{aligned} \tag{54}$$

Finally, we observe from (52) and (54) that all outage events in (50) yield higher outage exponents than $\mathcal{E}_{h,\overline{m}}$ or $\mathcal{E}_{g,\overline{m},0}$. Therefore, we eventually conclude that

$$P_{\text{out}}^{\text{JE}} \dot{\leq} P(\mathcal{E}_{h,\overline{m}}) + P(\mathcal{E}_{g,\overline{m},0}) \doteq \rho^{-\min(d_{h,\overline{m}}(R), d_{g,\overline{m},0}(R))},$$

and the proof of DRT lower-bound is established.

(2) DRT Upper-bound: We start from the lower-bound of $P_{\text{out}}^{\text{JE}}$ defined in (34). For a fixed rate R, it can be rephrased by

$$\begin{aligned} P_{\text{out}}^{\text{JE}} &\dot{\geq} P\Big(\sum_{k=1}^{M} \frac{1}{1+\rho\lambda_{h,k}} + \sum_{k=1}^{M} \frac{1}{\rho\lambda_{y,k}^{-1}(1+\rho\lambda_{g,k})} \\ &\qquad > \frac{N_S}{1-\epsilon} 2^{-\frac{\eta R}{N_S}} + M - N_S\Big) \\ &\doteq P\Big(\sum_{k=1}^{M} \frac{1}{1+\rho^{1-\alpha_k}} \\ &\qquad + \sum_{k=1}^{M} \frac{1}{\rho^{1-\beta_k} + \rho^{-(1-\alpha_k)} + \rho^{\alpha_k-\beta_k}} > (m_\epsilon)^+\Big), \end{aligned} \tag{55}$$

where $m_\epsilon \triangleq \frac{N_S}{1-\epsilon} 2^{-\frac{\eta R}{N_S}} + M - N_S$. Asymptotically, the following equality holds:

$$\frac{1}{\rho^{1-\beta_k} + \rho^{-(1-\alpha_k)} + \rho^{\alpha_k-\beta_k}} \doteq \begin{cases} 1 & \text{if } \alpha_k < 1 \text{ and } \beta_k > 1 \\ 0 & \text{if } \alpha_k > 1 \text{ or } \beta_k < 1 \end{cases} \tag{56}$$

for $k=1,\ldots,M$, which is exponentially equivalent to (49). Therefore, the remaining proof simply follows the previously studied DRT lower-bound by replacing m with m_ϵ. Finally, we have

$$P_{\text{out}}^{\text{JE}} \dot{\geq} P(\mathcal{E}_{h,\overline{m}_\epsilon}) + P(\mathcal{E}_{g,\overline{m}_\epsilon,0}) \doteq \rho^{-\min(d_{h,\overline{m}_\epsilon}(R), d_{g,\overline{m}_\epsilon,0}(R))},$$

where $\overline{m}_\epsilon \triangleq \lceil (m_\epsilon)^+ \rceil$. As long as $N_S 2^{-\frac{\eta R}{N_S}} \notin \mathbb{N}$ is non-integer, the constant ϵ can be chosen such that $\overline{m}_\epsilon = \overline{m}$. Therefore, the upper and lower bounds are tight. However, when $N_S 2^{-\frac{\eta R}{N_S}} \in \mathbb{N}$ takes an integer value, the outage exponent obeys a slightly weaker upper-bound with $\overline{m}_\epsilon = \lfloor (m+1)^+ \rfloor$, and the proof is concluded. ∎

[6] The p.d.f. is slightly different from [31], since the eigenvalue ordering is reversed.

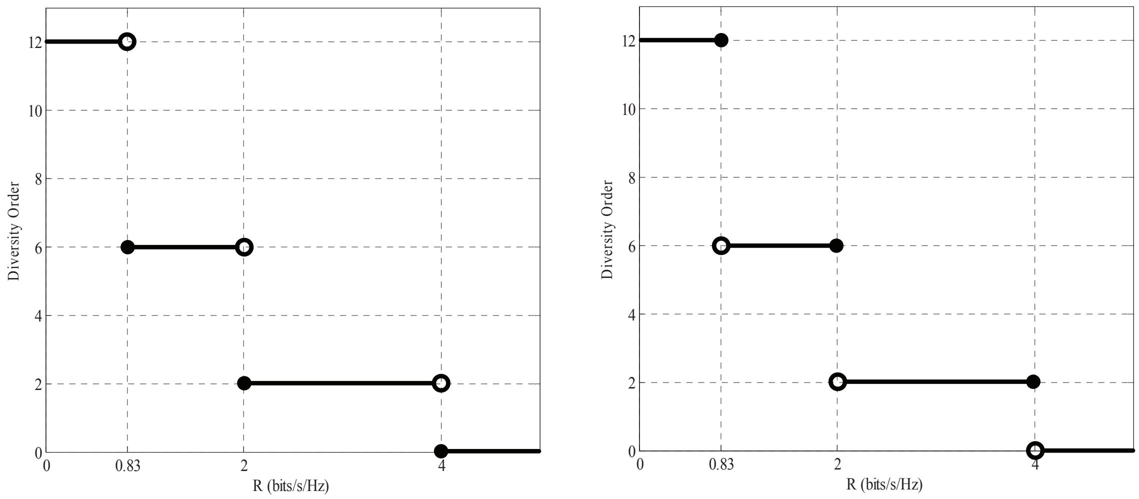

(a) DRT lower-bound

(b) DRT upper-bound

Fig. 2. DRT lower and upper bounds of the MMSE transceiver in $4 \times 4 \times 3$ MIMO AF relaying systems with $\eta = 2$

Our result in Theorem 6 confirms and complements the earlier work on DMT in Theorem 2. When the rate is high, i.e., $R > \frac{N_S}{\eta} \log N_S$ or $\lceil (m)^+ \rceil = \lfloor (m+1)^+ \rfloor = 1$, both the DMT and the DRT yield the same diversity order. Therefore, the DMT for the MMSE transceiver in Theorem 2 is already tight for all rates above a threshold $R > \frac{N_S}{\eta} \log N_S$. On the contrary, Theorem 6 demonstrates that as the rate becomes lower, a higher diversity gain is actually achievable than the one predicted by the DMT. In particular, when $R < \frac{N_S}{\eta} \log \frac{N_S}{N_S - 1}$, i.e., $\lceil (m)^+ \rceil = \lfloor (m+1)^+ \rfloor = M$, the MMSE transceivers even exhibit the ML-like performance with full diversity order $d(R) = N_R \min(N_S, N_D)$. It is also interesting to observe that when the rate is sufficiently small, a certain diversity gain is still achievable even in the case of $N_S > \min(N_R, N_D)$, which is often overlooked in conventional works for linear transceivers in MIMO relaying systems [3] [4] [6].

A careful examination of the bounds in (45) reveals that the upper-bound is left-continuous while the lower-bound is right-continuous at the discontinuity points. To help readers understand better, we take an example in Figure 2 which shows the DRT performance of the MMSE transceiver in $4 \times 4 \times 3$ MIMO AF relaying channels. As seen, two bounds in (45) are very tight against each other except for its discrepant points. It is also confirmed from the figure that various diversity gains, up to the full diversity order, are achievable by adjusting the transmit rate. As shown in the following, however, this may not be the case when the naive-MMSE scheme is adopted.

Theorem 7: Define (N, Y, Z) be the ordered version of (N_S, N_R, N_D) with $N \le Y \le Z$. Then, for the fixed spectral efficiency R, the DRT of the naive-MMSE over $N_S \times N_R \times N_d$ MIMO AF relaying channels, constrained to use the joint encoding scheme, is given by

$$D_{\text{N-ME}}\left(\lceil (n)^+ \rceil\right) \le d_{\text{N-ME}}(R) \le D_{\text{N-ME}}\left(\lfloor (n+1)^+ \rfloor\right), \quad (57)$$

where $n \triangleq N_S 2^{-\frac{2R}{N_S}} + N - N_S$ and

$$D_{\text{N-ME}}(i) \triangleq i(Y - N + i) - \left\lfloor \frac{\left[(i - (Z - Y))^+\right]^2}{4} \right\rfloor.$$

The upper and lower bounds of (57) always meet except for some discontinuity points, i.e., $n = 1, 2, \ldots, N_s$.

Proof: We prove the theorem by developing the DRT lower-bound of the naive-MMSE with the joint encoding scheme. As mentioned previously, the naive relay channel is asymptotically approximated to the Rayleigh product channel. Thus, applying the similar argument as in (46) and (47), we can write the outage upper-bound as

$$P_{\text{out}} \le P\Big(-\frac{N_S}{\eta} \log\Big(\frac{1}{N_S} \text{Tr}[(\rho \mathbf{H}^H \mathbf{G}^H \mathbf{G} \mathbf{H} + \mathbf{I}_{N_S})^{-1}]\Big) < R\Big)$$
$$\doteq P\Big(\sum_{k=1}^{N} \frac{1}{1 + \rho^{1-\gamma_k}} > (n)^+\Big),$$

where $n \triangleq N_S 2^{-\frac{\eta R}{N_S}} + N - N_S$. Let us define events $\mathcal{E}_i = \{\gamma_i > 1 > \gamma_{i+1}\}$ for all i. Then, for large ρ, the following approximation holds:

$$P\left(\sum_{k=1}^{N} \frac{1}{1 + \rho^{1-\gamma_k}} > (n)^+\right) \approx \bigcup_{i=\overline{n}}^{N} \mathcal{E}_i \le \sum_{i=\overline{n}}^{N} P(\mathcal{E}_i),$$

where $\overline{n} \triangleq \lceil (n)^+ \rceil$.

We now define $P(\mathcal{E}_i) \doteq \rho^{-d_i(R)}$ for $i = 1, \ldots, N$. Then, using the pdf $f(\mathbf{c}) \doteq \rho^{-\theta(\mathbf{c})}$ of a random vector $\mathbf{c} = [\gamma_1, \ldots, \gamma_N]$ given in Appendix D, we obtain

(a) for $N_R = N$,

$$\begin{aligned} d_i(R) &= \inf_{\mathbf{c} \in \mathcal{E}_i, \forall \gamma_k > 0} \theta_1(\mathbf{c}) \\ &= i(\min(N_S, N_D) - N_R + i) \\ &\quad - \left\lfloor \frac{\left[(i - |N_S - N_D|)^+\right]^2}{4} \right\rfloor \end{aligned}$$

(b) for $N_D \le N_R \le N_S$ or $N_S \le N_R \le N_D$,

$$\begin{aligned} d_i(R) &= \inf_{\mathbf{c}\in\mathcal{E}_i,\forall\gamma_k>0} \theta_2(\mathbf{c}) \\ &= i(N_R - \min(N_S,N_D)+i) \\ &\quad - \left\lfloor \frac{\left[(i-|\max(N_S,N_D)-N_R|)^+\right]^2}{4} \right\rfloor \end{aligned}$$

(c) for $N_D \le N_S < N_R$ or $N_S \le N_D < N_R$,

$$\begin{aligned} d_i(R) &= \inf_{\mathbf{c}\in\mathcal{E}_i,\forall\gamma_k>0} \theta_3(\mathbf{c}) \\ &= i(\max(N_S,N_D) - \min(N_S,N_D)+i) \\ &\quad - \left\lfloor \frac{\left[(i-|N_R-\min(N_S,N_D)|)^+\right]^2}{4} \right\rfloor. \end{aligned}$$

Finally, combining the above three, we arrive at $d_i(R) = D_{\text{N-ME}}(i)$. Thus, we can eventually conclude that $\sum_{i=\overline{n}}^{N} P(\mathcal{E}_i) \doteq \rho^{-d_{\overline{n}}(R)}$, and the DRT lower-bound is established. For the DRT upper-bound, the proof follows as an immediate corollary from the previous results in Theorem 6; thus is omitted. ■

Some remarks can be made from Theorem 7 about DRT performance of the naive-MMSE scheme. First, the upper and lower bounds in (57) are tight except for some inconsistent points. In addition, the DRT of the naive-MMSE does not depend on the antenna configuration (N_S, N_R, N_D), but only depends on its ordered triple (N, Y, Z).

Since $D_{\text{N-ME}}(i)$ is an increasing function of i, the maximum achievable diversity of the naive-MMSE is given by

$$NY - \left\lfloor \frac{\left[(N-Z+Y)^+\right]^2}{4} \right\rfloor,$$

when $\lceil (n)^+ \rceil = \lfloor (n+1)^+ \rfloor = N$ or $R < \frac{N_S}{\eta}\log\left(\frac{N_S}{N_S-1}\right)$. Now, we see that in order for the naive-MMSE to achieve the full-diversity order of MIMO AF relaying channels, the following two conditions must be fulfilled: $N_R \in \{N, Y\}$ and $N < Z - Y + 2$, which are not always the case in practice. Accordingly, regardless of the target rate R, the full-diversity order is not achievable in general with the naive-MMSE scheme. When the rate is high such that $R > \frac{N_S}{\eta}\log N_S$, i.e., $\lceil (n)^+ \rceil = \lfloor (n+1)^+ \rfloor = 1$, the diversity order is the same as one predictable by the DMT in Theorem 4.

VI. Future Work: Extension to Multi-hop Scenarios

When the communication range between the source and the destination is very long, which is often the case in rural area, multi-hop relaying architecture may be useful. Therefore, analytical study on the performance of multi-hop MIMO AF relaying channels is also a topic of great interest. In this section, we show that our ECD framework in Lemma 1 and 2 can be generalized to L-hop channels, from which we catch a glimpse of our future work.

Figure 3 illustrates a system model for L-hop MIMO relaying channels where $\mathbf{H}_l \in \mathbb{C}^{N_{R_l}\times N_{R_{l-1}}}$ indicates the l-th hop channel matrix for $l = 1,\dots,L$, and $\mathbf{Q}_l$ and $\mathbf{y}_{R_l}$ represent the linear transceiver and the received signal at the l-th relay for $l = 1,\dots,L-1$, respectively. Here, it is assumed that the l-th relay is equipped with N_{R_l} number of antennas. Then, we have

$$\mathbf{y}_{R_l} = \mathbf{A}_l\mathbf{x} + \mathbf{v}_l, \quad \text{for} \quad l = 1,\dots,L-1$$

where $\mathbf{A}_l \in \mathbb{C}^{N_{R_l}\times N_S}$ is the equivalent MIMO channel matrix from the source to the l-th hop and $\mathbf{v}_l$ is the equivalent noise vector given by

$$\begin{aligned} \mathbf{A}_1 &= \mathbf{H}_1, \quad \mathbf{A}_l = \prod_{i=1}^{l-1}\mathbf{H}_{i+1}\mathbf{Q}_i\mathbf{H}_i, \quad l = 2,\dots,L-1 \\ \mathbf{v}_1 &= \mathbf{n}_{R_1}, \quad \mathbf{v}_l = \sum_{j=1}^{l-1}\Big(\prod_{i=j}^{l-1}\mathbf{H}_{i+1}\mathbf{Q}_i\mathbf{n}_{R_j}\Big) + \mathbf{n}_{R_l}, \\ &\qquad\qquad\qquad\qquad\qquad l = 2,\dots,L-1. \end{aligned}$$

Here, $\mathbf{n}_{R_j}$ indicates the noise vector at the j-th relay and for matrices $\mathbf{X}_i$, $\prod_{i=k}^{l}\mathbf{X}_i = \mathbf{X}_l\cdots\mathbf{X}_k$. Then, denoting by $\mathbf{y}_D$ the received signal at the destination, we obtain the final observation vector as

$$\hat{\mathbf{x}} = \mathbf{W}\mathbf{y}_D = \mathbf{W}(\mathbf{H}_L\mathbf{Q}_{L-1}\mathbf{y}_{R_{L-1}} + \mathbf{n}_D).$$

With this signal model, first we can claim that the optimal matrix $\mathbf{Q}_l$ at the l-th relay equals $\mathbf{Q}_l = \mathbf{B}_l\mathbf{L}_l$ for $l = 1,\dots,L-1$ where $\mathbf{B}_l \in \mathbb{C}^{N_{R_l}\times N_{R_S}}$ is an arbitrary matrix and $\mathbf{L}_l \in \mathbb{C}^{N_{R_S}\times N_{R_l}}$ is the MMSE estimator of the input signal $\mathbf{x}$, which is given by

$$\mathbf{L}_l = (\rho\mathbf{A}_l^H\mathbf{R}_{v_l}^{-1}\mathbf{A}^H + \rho^{-1}\mathbf{I})^{-1}\mathbf{A}_l^H\mathbf{R}_{v_l}^{-1}$$

with the effective noise covariance $\mathbf{R}_{v_l} \triangleq E[\mathbf{v}_l\mathbf{v}_l^H]$. The result is simply obtained from Lemma 1 by replacing $\mathbf{P}$ with $(\rho\mathbf{A}_l^H\mathbf{R}_{v_l}^{-1}\mathbf{A}^H + \rho^{-1}\mathbf{I})^{-1}$ and $\mathbf{H}^H$ with the effective channel at the l-th relay with noise whitening, i.e., $\mathbf{A}_l^H\mathbf{R}_{v_l}^{-1}$.

For given the relay receiver $\mathbf{L}_l$, we now define $\mathbf{y}_l$ as the relay receiver output signal, i.e., $\mathbf{y}_l = \mathbf{L}_l\mathbf{y}_{R_l}$ at the l-th relay as shown in Figure 3. Let $\mathbf{R}_{y_l} = E[\mathbf{y}_l\mathbf{y}_l^H] \in \mathbb{C}^{N_S\times N_S}$ be the covariance matrix of $\mathbf{y}_l$ and define its eigenvalue decomposition as $\mathbf{R}_{y_l} = \mathbf{U}_{h_l}\mathbf{\Lambda}_{y_l}\mathbf{U}_{h_l}^H$ where $\mathbf{\Lambda}_{y_l} \in \mathbb{C}^{N_S\times N_S}$ represents a square diagonal matrix with eigenvalues $\lambda_{y_l,k}$ for $k = 1,\dots,N_S$ arranged in descending order. Then, we can show that the ECD property in Section III is also valid in the general L-hop channels.

Lemma 5: For given the relay matrices $\mathbf{Q}_l = \mathbf{B}_l\mathbf{L}_l$ for $l = 1,\dots,L-1$, the error covariance matrix of general L-hop MIMO AF relaying systems is given by

$$\begin{aligned} \mathbf{R}_e &= (\mathbf{H}_1^H\mathbf{H}_1 + \rho^{-1}\mathbf{I}_{N_S})^{-1} \\ &+ \sum_{l=1}^{L-1}\widetilde{\mathbf{U}}_{h_l}\big(\widetilde{\mathbf{U}}_{h_l}^H\mathbf{B}_l^H\mathbf{H}_{l+1}^H\mathbf{H}_{l+1}\mathbf{B}_l\widetilde{\mathbf{U}}_{h_l} + \widetilde{\mathbf{\Lambda}}_{y_l}^{-1}\big)^{-1}\widetilde{\mathbf{U}}_{h_l}^H, \end{aligned} \quad (58)$$

where $\widetilde{\mathbf{U}}_{h_l} \in \mathbb{C}^{N_S\times M_l}$ is a matrix constructed by the first $M_l = \min(N_S, N_{R_1},\cdots,N_{R_l})$ columns of $\mathbf{U}_{h_l}$ and $\widetilde{\mathbf{\Lambda}}_{y_l}$ indicates the $M_l\times M_l$ upper-left submatrix of $\mathbf{\Lambda}_{y_l}$.

Proof: See Appendix E. ■

Thus, under the MMSE strategy with full CSI relays, the optimal precoder $\mathbf{B}_l$ of the l-th relay is generally written by $\mathbf{B}_l = \widetilde{\mathbf{U}}_{h_{l+1}}\mathbf{\Phi}_l\widetilde{\mathbf{U}}_{h_l}^H$ with a diagonal matrix $\mathbf{\Phi}_l \in \mathbb{C}^{M_l\times M_l}$

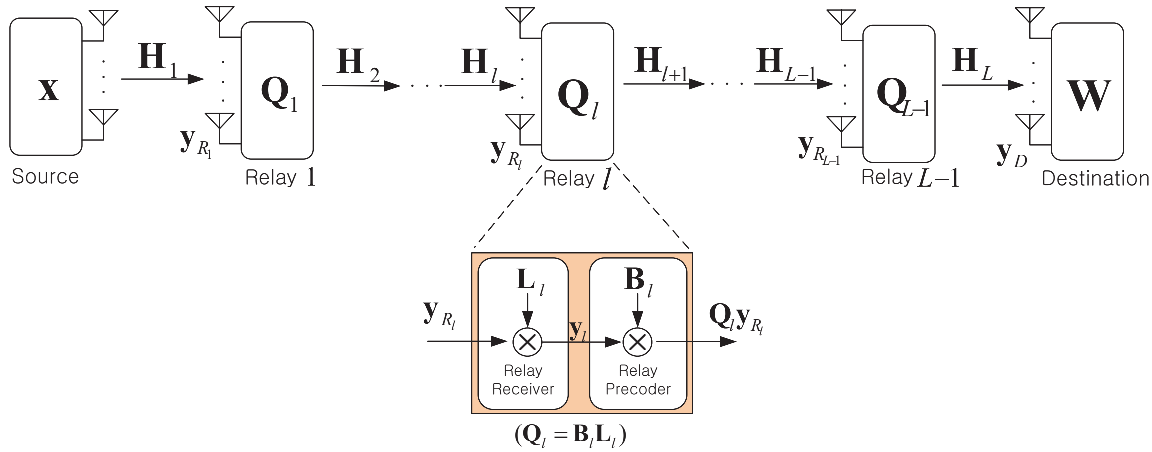

Fig. 3. System model for general L-hop MIMO AF relaying channels with linear transceivers.

whose elements are chosen to satisfy the l-th relay power constraint, i.e., Tr$(\mathbf{\Phi}_l\widetilde{\mathbf{\Lambda}}_{y_l}\mathbf{\Phi}_l^H) \leq P_{R_l}$ while minimizing the total MSE, i.e., Tr$(\mathbf{R}_e)$. It is generally difficult to identify the optimal $\mathbf{\Phi}_l$ due to non-convexity of the problem, but we can verify that any power allocation strategies in $\mathbf{\Phi}_l$ do not affect the diversity order. Therefore, the generalized ECD in (58) offeres a simple closed-form solution for the l-th relay transceiver as $\mathbf{Q}_l = \gamma \mathbf{V}_{h_{l+1}}\widetilde{\mathbf{U}}_{h_l}^H\mathbf{L}_l$ whose diversity order is the same as the solution obtained by some iterative methods proposed in [34].[7] It is also shown that we can characterize the maximum achievable diversity order even without knowing the exact form of the optimal solution.

However, the analysis will be more challenging compared to the two-hop MMSE cases, because the parameters $\lambda_{y_l,k}$'s, which play an important role for analysis, incorporates all previous channel components in $\mathbf{H}_1, \ldots, \mathbf{H}_{l-1}$, and thus form complicated structures. In addition, there exist abundant cases of naive schemes according to the CSI level at each relay, most of which are difficult to analyze due to the channel non-diagonalizing structure. Therefore, detailed analysis goes beyond the scope of this paper, and thus will be studied in our future work.

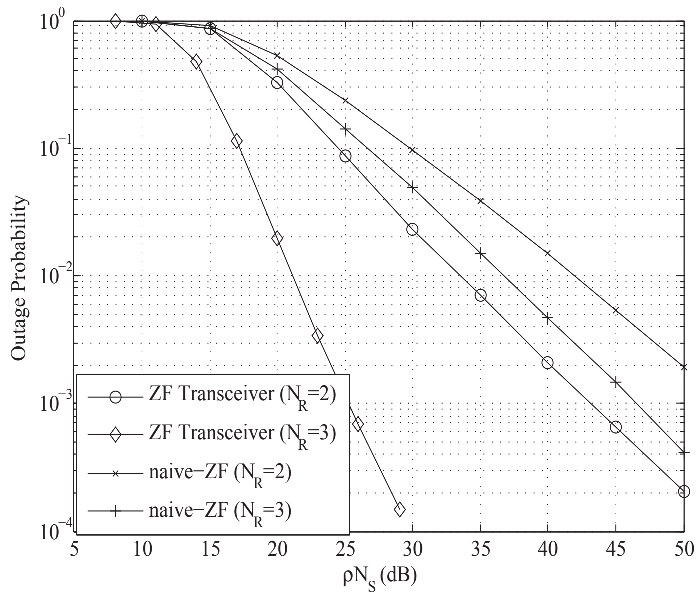

Fig. 4. Outage probabilities of ZF schemes under the JE with $N_S = N_D = 2$ and $R = 3.32$ bits/s/Hz

VII. Numerical Results

The goal of this section is to demonstrate the accuracy of our analysis and provide several interesting observations through numerical simulations. Throughout the section, we assume the two-hop half-duplex relaying systems ($\eta = 2$) while considering both the joint encoding (JE) and separate encoding (SE) schemes. Figure 4 compares two ZF schemes (the ZF transceiver and the naive-ZF) with the JE. It is seen that the ZF transceiver not only obtains the power gain about 10 dB over the naive-ZF, but also achieves a diversity gain when $N_R > N_D$. This result implies that a proper transceiver design assisted by the CSI at the relay is important to fully exploit the potential diversity of the MIMO AF relaying systems. The figure also confirms that our DMT analysis in Theorem 3 and 5 accurately predicts the numerical performance of the ZF schemes.

Figure 5 illustrates the case of $2 \times 2 \times 2$ systems with $R = 0.42$ and 2 bits/s/Hz. Here, *"Optimal"* exhibits the outage probability of the MIR transceiver described in (18). As predicted by Theorem 6, we observe that when the coding is applied jointly across antennas, the MMSE transceiver shows near optimal performance as the rate becomes smaller, while the ZF transceiver exhibits parallel waterfall error curves regardless of the coding scheme and the code rate as predicted by the DMT in Theorem 3. Similar observation can be made in Figure 6 which compares the outage performance of the naive-MMSE and the MMSE transceiver in $3 \times 3 \times 2$ systems with $R = 0.39$ bits/s/Hz. It is shown that while the SE schemes

[7] Here, γ is a power normalizing constant to satisfy the power constraint. In this case, we can set $\gamma = \sqrt{\frac{P_{R_l}}{M_l}}$ since we have Tr$(\mathbf{\Phi}_l\widetilde{\mathbf{\Lambda}}_{y_l}\mathbf{\Phi}_l^H) \leq$ Tr$(\mathbf{\Phi}_l\mathbf{\Phi}_l^H)$ as shown in Lemma 3.

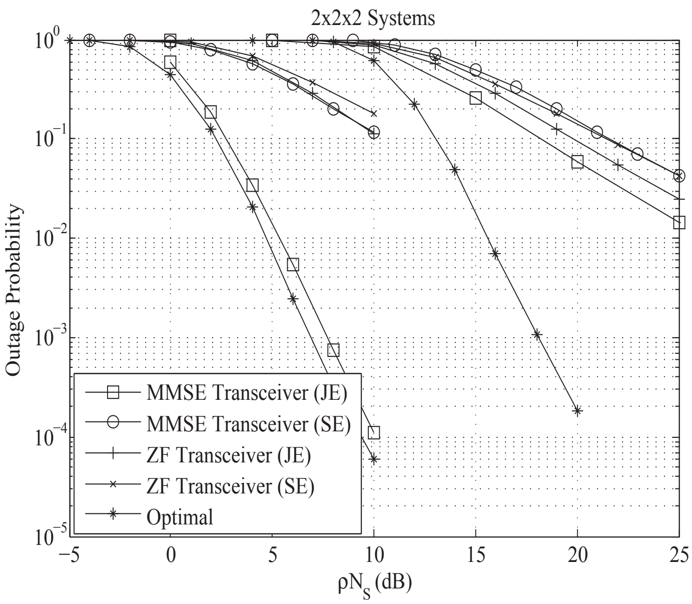

Fig. 5. Outage probabilities of MMSE and ZF transceivers with $R = 0.42$ and 2 bits/s/Hz (left to right)

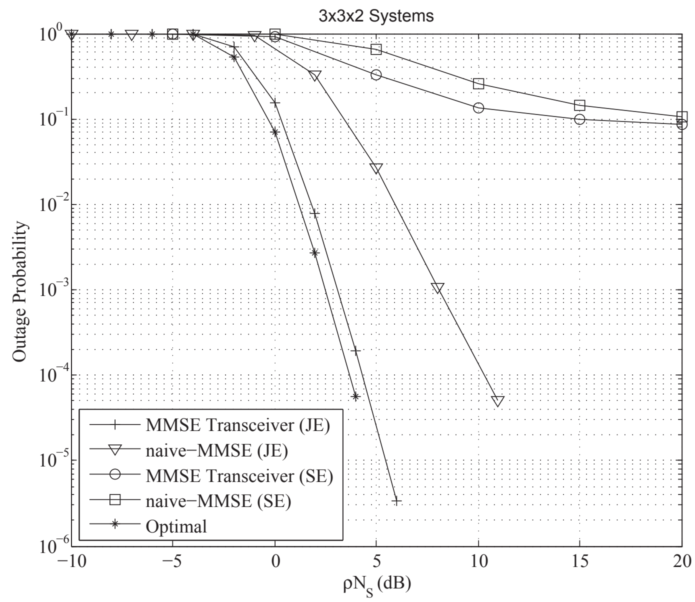

Fig. 6. Outage probabilities of the MMSE schemes with $R = 0.39$ bits/s/Hz

experience outage floor due to lack of spatial dimension at the destination, the MMSE schemes combined with the JE still enjoy a substantial performance advantage. In fact, this observation is quite antithetic to the common assumption $N_S \leq \min(N_R, N_D)$ which has usually been adopted in MMSE-based MIMO relaying systems [4] [35] [36]. It is also interesting to observe that unlike the MMSE transceiver, the naive-MMSE does not achieve the full-diversity order, even if the rate is sufficiently small. This is easily inferred from Theorem 6 and 7 since the DRT of the naive MMSE exhibits only $d_{\text{N-ME}}(0.39) = 5$ due to the penalty term in (57), while the MMSE transceiver yields the full diversity $d_{\text{ME}}(0.39) = 6$.

Meanwhile, it is sometimes the case that adding antennas at each node may be more convenient than insisting on high-complexity receiver processing at the destination [31]. Let us consider the outage curves in Figure 7. Suppose that we want to achieve the rate $R = 2$ bits/s/Hz at the block error rate 10^{-3} with SNR $\rho N_S = 18$ dB. Figure 7 shows that this target performance is achieved by the $2 \times 2 \times 2$ optimal scheme, but obviously not via $2 \times 2 \times 2$ MMSE scheme. One way to improve the performance of the MMSE scheme is to increase the number of antennas at the relay, since we know that additional antennas at the relay leads to additional DMT advantage (this is not the case in the naive-MMSE). A big merit of this method is that the target performance can be achieved even with the SE. If the JE is available, it may also be possible to improve the performance by increasing the data streams because the per-stream rate becomes small as N_S goes to high. For example, it is shown that the MMSE transceiver in $3 \times 3 \times 3$ and $4 \times 4 \times 4$ systems attains substantial performance gain over one in $2 \times 2 \times 2$ systems.

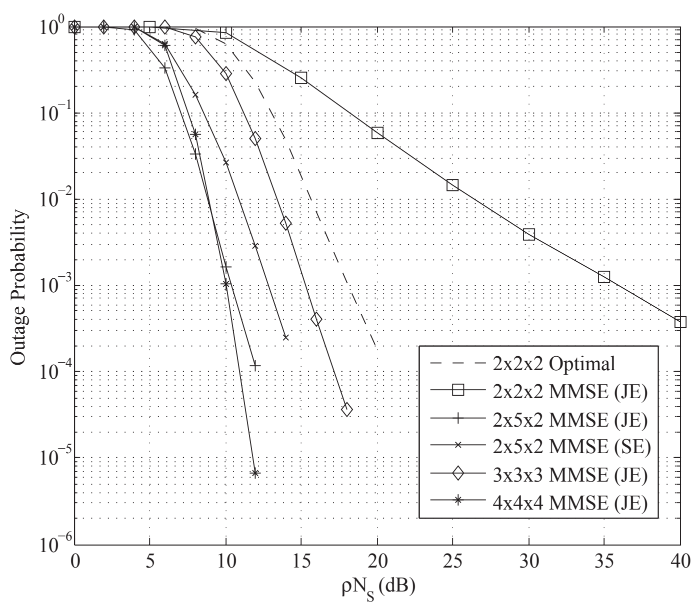

Fig. 7. Outage probabilities of the optimal and MMSE transceivers with $R = 2$ bits/s/Hz

Figure 8 presents the outage probability of the MMSE transceiver for $3 \times 3 \times 4$ and $4 \times 3 \times 3$ systems with various rates. We see that while the performance of $4 \times 3 \times 3$ systems may be poor and even floored at high rates, it shows similar performance to $3 \times 3 \times 4$ systems as the rate becomes smaller. This result implies that when the rate is sufficiently small, increasing the data streams at the source (base-station) is as effective as increasing the antennas at the destination (user). This result is particularly useful when the mobile users suffer from antenna space limitation.

Finally, in Figure 9, we investigate performance trends of the MMSE transceiver in $4 \times 4 \times 3$ systems with discontinuity rate points. As illustrated in Figure 2, in this case, the discontinuity points occur at $R = 0.83$, 2, and 4 bits/s/Hz. We confirm from Figure 9 that the actual diversity orders of

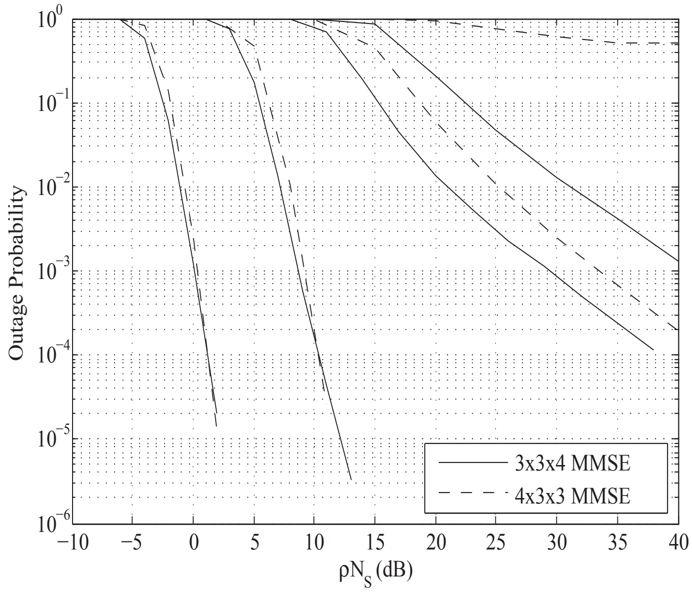

Fig. 8. Outage probabilities of the MMSE transceiver under the JE with $R = 0.3$, 1.2, 3, and 5 bits/s/Hz (left to right)

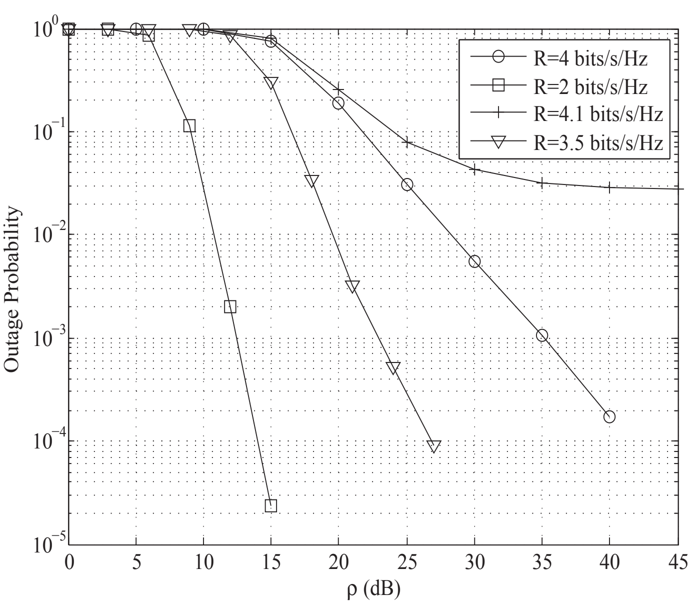

Fig. 9. Outage probabilities of the MMSE transceiver in $4 \times 4 \times 3$ systems under the JE with discontinuity rate points.

$R = 2$ and 4 cases lie between the analytical upper and lower bounds, but they do not seem to match with either the upper or lower bounds. In contrast, it is shown that the cases of $R = 3.5$ and 4.1 bits/s/Hz being on the continuous rate points draw exactly the same diversity order as what we derived in Theorem 6.

VIII. Conclusion

In this paper, we provided comprehensive analysis on the diversity order of various transceiving schemes in MIMO AF relaying systems. We first presented the ECD-based design framework for transceiver optimization in terms of the ZF, MMSE, and MIR criteria, and then provided two different types of asymptotic performance analysis. In the first part of the analysis, we studied the DMT performance of the ZF and MMSE schemes. While the DMT analysis accurately predicts their diversity performance for the positive multiplexing gain, it was shown that the MMSE schemes are very unpredictable via DMT when the rate is finite. In the second part of the analysis, we highlighted this rate-dependent behavior of the MMSE-based designs and characterized their diversity at all finite rates. It is especially interesting to observe that the MMSE transceiver exhibits the ML-like performance as the rate becomes smaller, but the full-diversity order is not guaranteed in the naive-MMSE, even if the rate is arbitrarily small. Through the designs and the analysis on both the DMT and the DRT, the paper offered complete understanding on the diversity order of the MIMO AF relaying systems. Finally, simulation results confirmed our analysis. Extensions to multi-hop channels will also be an attractive area for future works.

Appendix A
Achievability Proof of $d^*(r)$

From the results in (17) and (18), the MIR problem in (18) is equivalently changed to

$$\begin{aligned}\mathcal{I}(\mathbf{\Phi}) &= \max_{\mathbf{\Phi}} \frac{1}{\eta} \log \frac{\left|\mathbf{I}_M + \rho\widetilde{\mathbf{\Lambda}}_h\right| \left|\mathbf{I}_M + \mathbf{\Phi}^H\widetilde{\mathbf{\Lambda}}_g\mathbf{\Phi}\right|}{\left|\mathbf{I}_M + \rho\widetilde{\mathbf{\Lambda}}_h + \mathbf{\Phi}^H\widetilde{\mathbf{\Lambda}}_g\mathbf{\Phi}\right|} \\ & \quad s.t. \;\; \text{Tr}(\mathbf{\Phi}^H\mathbf{\Phi}) \le P_R = N_S\rho.\end{aligned}$$

Instead of the optimal solution presented in Section III-C, let us consider a suboptimal $\mathbf{\Phi} = \sqrt{\rho}\mathbf{I}$ which satisfies the above power constraint. Then, we obtain the MI lower-bound as follows:

$$\begin{aligned}\mathcal{I} &\ge \frac{1}{\eta} \log \frac{\left|\mathbf{I}_M + \rho\widetilde{\mathbf{\Lambda}}_h\right| \left|\mathbf{I}_M + \rho\widetilde{\mathbf{\Lambda}}_g\right|}{\left|\mathbf{I}_M + \rho\widetilde{\mathbf{\Lambda}}_h + \rho\widetilde{\mathbf{\Lambda}}_g\right|} \\ &= \frac{1}{\eta} \log \frac{\prod_{k=1}^M \left[(1+\rho^{1-\alpha_k})(1+\rho^{1-\beta_k})\right]}{\prod_{k=1}^M (1+\rho^{1-\alpha_k}+\rho^{1-\beta_k})} \\ &\doteq \frac{1}{\eta} \log \Big(\prod_{k=1}^M \rho^{\max(0,1-\alpha_k,1-\beta_k,2-\alpha_k-\beta_k)} \\ &\qquad \times \rho^{-\max(0,1-\alpha_k,1-\beta_k)} \Big) \\ &= \frac{1}{\eta} \log \Big(\prod_{k=1}^M \rho^{\min[(1-\alpha_k)^+,(1-\beta_k)^+]} \Big),\end{aligned}$$

where α_k and β_k are defined in (36), and setting the target rate as $R(\rho) = r \log \rho$, it follows

$$\begin{aligned}P_{\text{out}} &\dot{\le} P\Big(\frac{1}{\eta} \log \big(\prod_{k=1}^M \rho^{\min[(1-\alpha_k)^+,(1-\beta_k)^+]} \big) < R(\rho) \Big) \\ &= P\Big(\sum_{k=1}^N \min[(1-\alpha_k)^+,(1-\beta_k)^+] < \eta r \Big) \\ &= P\left(\mathcal{E}\right)\end{aligned}$$

where $\mathcal{E} = \{\sum_{k=1}^{N} \min[(1-\alpha_k)^+, (1-\beta_k)^+] < \eta r\}$ denotes the outage event. The second equality is due to the fact that we have $\rho\lambda_{g,k} = \rho^{1-\beta_k} = 0$, i.e., $\beta_k > 1$ for $k = N+1, \ldots, M$. Now, defining $P(\mathcal{E}) \doteq \rho^{-d(r)}$ and applying the Varadhan's lemma [31] [12] by using the pdfs of random vectors $\mathbf{a} = [\alpha_1, \ldots, \alpha_M]$ and $\mathbf{b} = [\beta_1, \ldots, \beta_{L=\min(N_R,N_D)}]$ given in (51) and (53), we obtain the outage exponent as

$$\begin{aligned} d(r) &\doteq \inf_{\{\mathbf{a},\mathbf{b}\}\in\mathcal{E},\forall\alpha_k>0,\forall\beta_k>0} \sum_{i=1}^{M}(N_S+N_R-2i+1)\alpha_i \\ &\qquad + \sum_{i=1}^{L}(N_R+N_D-2i+1)\beta_i, \\ &= \min\Big(\sum_{i=\eta r+1}^{M}(N_S+N_R-2i+1), \\ &\qquad \sum_{i=\eta r+1}^{L}(N_R+N_D-2i+1)\Big) \\ &= (N_R-\eta r)(\min(N_S,N_D)-\eta r), \end{aligned}$$

which amounts to the optimal DMT, and thus the proof is completed.

Appendix B
Proof of Lemma 3

From the definition of $\mathbf{R}_y$ in (7), it follows

$$\begin{aligned} \mathbf{R}_y &= (\mathbf{H}^H\mathbf{H}+\rho^{-1}\mathbf{I}_{N_S})^{-1}\mathbf{H}^H \\ &\qquad \times(\rho\mathbf{H}\mathbf{H}^H+\mathbf{I}_{N_S})\mathbf{H}(\mathbf{H}^H\mathbf{H}+\rho^{-1}\mathbf{I}_{N_S})^{-1} \\ &\overset{(a)}{=} \rho\mathbf{H}^H\mathbf{H}(\mathbf{H}^H\mathbf{H}+\rho^{-1}\mathbf{I}_{N_S})^{-1} \\ &= \rho(\mathbf{H}^H\mathbf{H}+\rho^{-1}\mathbf{I}_{N_S}-\rho^{-1}\mathbf{I}_{N_S}) \\ &\qquad \times(\mathbf{H}^H\mathbf{H}+\rho^{-1}\mathbf{I}_{N_S})^{-1} \\ &= \rho\mathbf{I}_{N_S}-(\mathbf{H}^H\mathbf{H}+\rho^{-1}\mathbf{I}_{N_S})^{-1}, \end{aligned} \quad (59)$$

where we obtain (a) by invoking the matrix inversion lemma. Since $\mathbf{A}-\mathbf{B}=\mathbf{C}$ implies that $\mathbf{A}\succeq\mathbf{C}$ for $\mathbf{A},\mathbf{B},\mathbf{C}\in\mathbb{S}^+$, it is obvious from (59) that $\mathbf{R}_y \preceq \rho\mathbf{I}_{N_S}$ and the proof is completed.

Appendix C
Proof of Lemma 4

By definition, $\mathbf{R}_z$ in (15) is rephrased as $\mathbf{R}_z = \rho\mathbf{I}_{N_S} + (\mathbf{H}^H\mathbf{H})^{-1}$, from which it is immediate that $\rho\mathbf{I}_{N_S} \preceq \mathbf{R}_z$. Meanwhile, since we have $\mathbf{H}^H\mathbf{H} \succeq \lambda_{h,N_S}\mathbf{I}_{N_S}$, one can easily show that $\mathbf{R}_z \preceq (\rho+\lambda_{h,N_S}^{-1})\mathbf{I}_{N_S} = \rho(1+\rho^{\alpha_{N_S}-1})\mathbf{I}_{N_S}$. From the Varadhan's lemma as in [12], it is also true that $(1+\rho^{\alpha_{N_S}-1}) \doteq \rho^0$, because α_{N_S} is smaller than 1 with probability 1. Therefore, we finally obtain $\rho\mathbf{I}_{N_S} \preceq \mathbf{R}_z \dot{\preceq} \rho\mathbf{I}_{N_S}$ and the proof is concluded.

Appendix D
Eigenvalue Distribution of Rayleigh Product Channels

Let $\mathbf{G}$,$\mathbf{H}$ be $n\times l$, $l\times m$ independent matrices with i.i.d. entries distributed as $\mathcal{CN}(0,1)$. We define a positive semi-definite matrix $\mathbf{A} = \mathbf{H}^H\mathbf{G}^H\mathbf{G}\mathbf{H}$ with eigenvalues $\lambda_{t,1} > \cdots > \lambda_{t,N}$ and $\gamma_k \triangleq -\log\lambda_{t,k}/\log\rho$ for $k=1,\ldots,N$. Then, denoting the pdf of a random vector $\mathbf{c} = [\gamma_1,\ldots,\gamma_N]$ as $f(\mathbf{c}) \doteq \rho^{-\theta(\mathbf{c})}$, the exponential order $\theta(\mathbf{c})$ is given as follows:

- When $l < \min(m,n)$,

$$\begin{aligned} \theta_1(\mathbf{c}) &= \sum_{k=1}^{l-|m-n|}\Big(\overline{n}+1-2k+\Big\lfloor\frac{l+k+|m-n|}{2}\Big\rfloor\Big)\gamma_k \\ &\qquad + \sum_{l-|m-n|+1}^{l}(\overline{n}+l+1-2k)\gamma_k \end{aligned} \quad (60)$$

  In this case, m and n can be exchanged by the reciprocity property of MIMO channels.

- When $n\le l\le m$ or $m\le l\le n$,

$$\begin{aligned} \theta_2(\mathbf{c}) &= \sum_{k=1}^{l-|m-n|}\Big(\overline{p}+1-2k+\Big\lfloor\frac{l+k+|m-n|}{2}\Big\rfloor\Big)\gamma_k \\ &\qquad + \sum_{l-|m-n|+1}^{\overline{p}}(\overline{n}+l+1-2k)\gamma_k \end{aligned} \quad (61)$$

- When $n\le m<l$ or $m\le n<l$,

$$\begin{aligned} \theta_3(\mathbf{c}) &= \sum_{k=1}^{\overline{q}-|l-\overline{p}|}\Big(\overline{p}+1-2k+\Big\lfloor\frac{\overline{q}+k+|l-\overline{p}|}{2}\Big\rfloor\Big)\gamma_k \\ &\qquad + \sum_{\overline{q}-|l-\overline{p}|+1}^{\overline{p}}(m+n+1-2k)\gamma_k \end{aligned} \quad (62)$$

where $\overline{p}\triangleq\min(m,n)$ and $\overline{q}\triangleq\max(m,n)$. For more details, please refer to [20].

Appendix E
Proof of Lemma 5

First, we define the MSE as $\|\mathbf{e}\|^2 \triangleq \|\hat{\mathbf{x}}-\mathbf{x}\|^2 = \|\hat{\mathbf{x}}-\mathbf{y}_{L-1}+\mathbf{y}_{L-1}-\mathbf{x}\|^2$. Recall that $\mathbf{y}_{L-1} = \mathbf{L}_{L-1}\mathbf{y}_{R_{L-1}}$ where $\mathbf{L}_{L-1}$ is the MMSE receiver for the input signal $\mathbf{x}$ and $\hat{\mathbf{x}} = \mathbf{W}(\mathbf{H}_L\mathbf{B}_{L-1}\mathbf{y}_{L-1}+\mathbf{n}_D)$ is a function of $\mathbf{y}_{L-1}$. Thus, from orthogonal principle, it follows $\|\mathbf{e}\|^2 = \|\hat{\mathbf{x}}-\mathbf{y}_{L-1}\|^2 + \|\mathbf{y}_{L-1}-\mathbf{x}\|^2$. Similarly, we show that the second term equals $\|\mathbf{y}_{L-1}-\mathbf{x}\|^2 = \|\mathbf{y}_{L-1}-\mathbf{y}_{L-2}\|^2 + \|\mathbf{y}_{L-2}-\mathbf{x}\|^2$. Therefore, by the chain rule, the MSE is equivalently decomposed to

$$\|\mathbf{e}\|^2 = \|\mathbf{y}_1-\mathbf{x}\|^2 + \sum_{i=1}^{L-2}\|\mathbf{y}_{i+1}-\mathbf{y}_i\|^2 + \|\hat{\mathbf{x}}-\mathbf{y}_{L-1}\|^2.$$

With this equation, it is shown that the destination receiver $\mathbf{W}$ in $\hat{\mathbf{x}}$ and the $(i+1)$-th relay receiver $\mathbf{L}_{i+1}$ in $\mathbf{y}_{i+1}$ are written by

$$\mathbf{W} = \mathbf{R}_{y_{L-1}}\mathbf{B}_{L-1}^H\mathbf{H}_L^H(\mathbf{H}_L\mathbf{B}_{L-1}\mathbf{R}_{y_{L-1}}\mathbf{B}_{L-1}^H\mathbf{H}_L^H+\mathbf{I}_{N_D})^{-1}$$

and $$\mathbf{L}_{i+1} = \mathbf{R}_{y_i}\mathbf{B}_i^H\mathbf{H}_{i+1}^H(\mathbf{H}_{i+1}\mathbf{B}_i\mathbf{R}_{y_i}\mathbf{B}_i^H\mathbf{H}_{i+1}^H+\mathbf{I}_{N_{R_{i+1}}})^{-1}$$

each of which amounts to the MMSE receiver for the virtual input signals $\mathbf{y}_{L-1}$ and $\mathbf{y}_i$, respectively. Thus, the remaining proof simply follows the previous result in Lemma 2 and we conclude the proof.

REFERENCES

[1] X. Tang and Y. Hua, "Optimal design of non-regenerative MIMO wireless relays," *IEEE Trans. Wireless Commun.*, vol. 6, pp. 1398–1407, April 2007.

[2] O. Munoz-Medina, J. Vidal, and A. Agustin, "Linear transceiver design in nonregenerative relays with channel state information," *IEEE Trans. Signal Process.*, vol. 55, pp. 2593–2604, June 2007.

[3] W. Guan and H. Luo, "Joint MMSE transceiver design in non-regenerative MIMO relay systems," *IEEE Commun. Lett.*, vol. 12, pp. 517–519, July 2008.

[4] C. Song, K.-J. Lee, and I. Lee, "MMSE based transceiver designs in closed-loop non-regenerative MIMO relaying systems," *IEEE Trans. Wireless Commun.*, vol. 9, pp. 2310–2319, July 2010.

[5] C. Xing, S. Ma, and Y.-C. Wu, "Robust joint design of linear relay precoder and destination equalizer for dual-hop amplify-and-forward MIMO relay systems," *IEEE Trans. Signal Process.*, vol. 58, pp. 2273–2283, April 2010.

[6] Y. Rong, X. Tang, and Y. Hua, "A unified framework for optimizing linear non-regenerative multicarrier MIMO relay communication systems," *IEEE Trans. Signal Process.*, vol. 57, pp. 4837–4851, December 2009.

[7] W. Zhang, U. Mitra, and M. Chiang, "Optimization of Amplify-and-Forward Multicarrier Two-Hop Transmission," *IEEE Trans. Commun*, March 2011.

[8] B. K. Chalise and L. Vandendorpe, "Performance analysis of linear receivers in a MIMO relaying system," *IEEE Commun. Lett.*, pp. 330–332, May 2009.

[9] R. H. Y. Louie, Y. Li, H. A. Suraweera, and B. Vucetic, "Performance analysis of beamforming in two hop amplify and forward relay networks with antenna correlation," *IEEE Trans. Wireless Commun.*, vol. 8, pp. 3132–3141, June 2009.

[10] C. Song, K.-J. Lee, and I. Lee, "Performance analysis of MMSE-based amplify and forward spatial multiplexing MIMO relaying systems," *IEEE Trans. Commun.*, vol. 59, pp. 3452–3462, December 2011.

[11] C. Song, K.-J. Lee, and I. Lee, "MMSE-based MIMO cooperative relaying systems: closed-form designs and outage behavior," *IEEE J. Sel. Areas Commun.*, vol. 30, pp. 1390–1401, September 2012.

[12] L. Zheng and D. N. C. Tse, "Diversity and multiplexing: a fundamental tradeoff in multiple-antennas channels," *IEEE Trans. Inf. Theory*, vol. 49, pp. 1073–1096, May 2003.

[13] K. Azarian, H. E. Gamal, and P. Schniter, "On the achievable diversity-multiplexing tradeoff in half-duplex cooperative channels," *IEEE Trans. Inf. Theory*, vol. 51, pp. 4152–4172, December 2005.

[14] S. Yang and J. C. Belfiore, "Optimal space-time codes for the MIMO amplify-and-forward cooperative channel," *IEEE Trans. Inf. Theory*, vol. 2, pp. 647–663, February 2007.

[15] S. Yang and J. C. Belfiore, "Towards the optimal amplify-and-forward cooperative diversity scheme," *IEEE Trans. Inf. Theory*, vol. 53, pp. 3114–3126, September 2007.

[16] M. Yuksel and E. Erkip, "Multiple-antenna cooperative wireless Systems: a diversity-multiplexing tradeoff perspective," *IEEE Trans. Inf. Theory*, vol. 53, pp. 3371–3393, October 2007.

[17] D. Gündüz, M. A. Khojastepour, A. Goldsmith, and H. V. Poor, "Multi-hop MIMO relay networks: diversity-multiplexing trade-off analysis," *IEEE Trans. Wireless Commun.*, vol. 9, pp. 1738–1747, May 2010.

[18] O. Lévêque, C. Vignat, and M. Yüksel, "Diversity-multiplexing tradeoff for the MIMO static half-duplex relay," *IEEE Trans. Inf. Theory*, vol. 56, pp. 3356–3368, July 2010.

[19] S. Loyka and G. Levin, "Diversity-multiplexing tradeoff in MIMO relay channels for a broad class of fading distributions," *IEEE Commun. Lett.*, vol. 14, pp. 327–329, April 2010.

[20] S. Yang and J. C. Belfiore, "Diversity-multiplexing tradeoff of double scattering MIMO channels," *IEEE Trans. Inf. Theory*, vol. 57, pp. 2027–2034, April 2011.

[21] A. Hedayat and A. Nosratinia, "Outage and diversity of linear receivers in flat-fading MIMO channels," *IEEE Trans. Signal Process.*, vol. 3, pp. 5868–5873, December 2007.

[22] A. H. Mehana and A. Nosratinia, "Diversity of MMSE MIMO receivers," *IEEE Trans. Inf. Theory*, vol. 58, pp. 6788–6805, November 2012.

[23] S. Boyd and L. Vandenberghe, *Convex Optimization*. The Edinburgh Building, Cambridge: Cambridge University Press, 2004.

[24] A. Paulraj, R. Nabar, and D. Gore, *Introduction to Space-Time Wireless Communications*. The Edinburgh Building, Cambridge, UK: Cambridge University Press, 2003.

[25] M. Joham, W. Utschick, and J. A. Nossek, "Linear transmit processing in MIMO communications systems," *IEEE Trans. Signal Process.*, vol. 53, pp. 2700–2712, August 2005.

[26] D. P. Palomar, J. M. Cioffi, and M. A. Lagunas, "Joint Tx-Rx beamforming design for multicarrier MIMO channels: a unified framework for convex optimization," *IEEE Trans. Signal Process.*, vol. 51, pp. 2381–2401, September 2003.

[27] N. Komaroff, "Bounds on eigenvalues of matrix products with an application to the algebraic riccati equation," *IEEE Trans. Autom. Control*, vol. 35, pp. 348–350, March 1990.

[28] S. Loyka and G. Levin, "On outage probability and diversity-multiplexing tradeoff in MIMO relay channels," *IEEE Trans. Commun.*, vol. 6, pp. 1731–1741, June 2011.

[29] C. Song and I. Lee, "Diversity analysis of coded beamforming in MIMO-OFDM amplify-and-forward relaying systems," *IEEE Trans. Wireless Commun.*, vol. 10, pp. 2445–2450, August 2011.

[30] E. Sengul, E. Akay, and E. Ayanoglu, "Diversity analysis of single and multiple beamforming," *IEEE Trans. Commun.*, vol. 54, pp. 990–993, June 2006.

[31] K. R. Kumar, G. Caire, and A. L. Moustakas, "Asymptotic performance of linear receivers in MIMO fading channels," *IEEE Trans. Inf. Theory*, vol. 55, pp. 4398–4418, October 2009.

[32] S. O. Gharan, A. Bayesteh, and A. K. Khandani, "On the diversity-multiplexing tradeoff in multiple-relay network," *IEEE Trans. Inf. Theorey*, vol. 55, pp. 5423–5444, December 2009.

[33] R. Pedarsani, O. Lévêque, and S. Yang, "On the DMT optimality of the rotate-and-forward scheme in a two-hop MIMO relay channel," in *Proc. 48th Annual Allerton Conference*, September 2010.

[34] Y. Rong and Y. Hua, "Optimality of diagonalization of multi-hop MIMO relays," *IEEE Trans. Wireless Commun.*, vol. 8, pp. 6068–6077, Dec 2009.

[35] R. Mo and Y. H. Chew, "MMSE-based joint source and relay precoding design for amplify-and-forward MIMO relay networks," *IEEE Trans. Wireless Commun.*, vol. 8, pp. 4668–4676, September 2009.

[36] F.-S. Tseng, "Linear MMSE transceiver design in amplify-and-forward MIMO relay systems," *IEEE Trans. Veh. Technol.*, vol. 59, pp. 754–765, February 2010.

Changick Song (S'09-M'13) received the B.S., M.S., and Ph.D. degrees in electrical engineering from Korea University, Seoul, Korea, in 2007, 2009, and 2012. He worked as a visiting researcher at University of Southern California, Los Angeles, CA, USA in 2009, and at Queens University, Kingston, ON, Canada in 2011. From September 2012 to April 2013, he was a Research Professor in Korea University and from May 2013 to August 2014, he was with the Communications and Signal Processing (CSP) Group at Imperial College, London, UK as a Postdoctoral Research Associate. In September 2014, he joined the faculty of Korea National University of Transportation, Chungju, Korea, where he is currently an Assistant Professor in the Department of Information and Communications Engineering. His research interest includes information theory and signal processing for wireless communications and security.

Cong Ling received the B.S. and M.S. degrees in electrical engineering from the Nanjing Institute of Communications Engineering, Nanjing, China, in 1995 and 1997, respectively, and the Ph.D. degree in electrical engineering from the Nanyang Technological University, Singapore, in 2005. He is currently a Senior Lecturer in the Electrical and Electronic Engineering Department at Imperial College London. His research interests are coding, signal processing, and security, especially lattices. Before joining Imperial College, he had been on the faculties of Nanjing Institute of Communications Engineering and King's College. Dr. Ling is an Associate Editor of IEEE Transactions on Communications. He has also served as an Associate Editor of IEEE Transactions on Vehicular Technology.